EUR 479.e

EUROPEAN ATOMIC ENERGY COMMUNITY - EURATOM

NEUTRON DISTRIBUTION IN A CRITICAL SLAB BY THE MULTIPLE COLLISION METHOD

by

T. ASAOKA (EURATOM) and
Y. NAKAHARA, K. SAITO
(Japan Atomic Energy Research Institute,
Tokai-mura, Ibaraki-ken, Japan)

1963

Joint Nuclear Research Center
Ispra Establishment - Italy

Reactor Physics Department
Applied Mathematical Physics

LEGAL NOTICE

This document was prepared under the sponsorship of the Commission of the European Atomic Energy Community (EURATOM).

Neither the EURATOM Commission, its contractors nor any person acting on their behalf :

1° — Make any warranty or representation, express or implied, with respect to the accuracy, completeness, or usefulness of the information contained in this document, or that the use of any information, apparatus, method, or process disclosed in this document may not infringe privately owned rights ; or

2° — Assume any liability with respect to the use of, or for damages resulting from the use of any information, apparatus, method or process disclosed in this document.

The authors' names are listed in alphabetical order.

This report can be obtained, at the price of Belgian Francs 70,— from : PRESSES ACADEMIQUES EUROPEENNES — 98, Chaussée de Charleroi, Brussels 6.

Please remit payments :

— to BANQUE DE LA SOCIETE GENERALE (Agence Ma Campagne) — Brussels — account No 964.558,

— to BELGIAN AMERICAN BANK AND TRUST COMPANY — New York — account No 121.86,

— to LLOYDS BANK (Foreign) Ltd. — 10 Moorgate — London E.C.2,

giving the reference : « EUR 479 . e — NEUTRON DISTRIBUTION IN A CRITICAL SLAB BY THE MULTIPLE COLLISION METHOD »

This document was duplicated on the basis of the best available copy.

Printed by IMPRIMERIE L. VANMELLE S.A., GHENT
Brussels, December 1963

EUR 479.e

NEUTRON DISTRIBUTION IN A CRITICAL SLAB BY THE MULTIPLE COLLISION METHOD by T. ASAOKA (EURATOM) and Y. NAKAHARA, K. SAITO (Japan Atomic Energy Research Institute, Tokai-mura, Ibaraki-ken, Japan)

European Atomic Energy Community — EURATOM
Joint Nuclear Research Center — Ispra Establishment (Italy)
Reactor Physics Department — Applied Mathematical Physics
Brussels, December 1963 — pages 47 — figures 8

The detailed distribution of monoenergetic neutrons, in a critical slab with finite thickness, is dealt with analytically by the multiple collision method or the random walk approach.

Under the assumption that the scattering of neutrons is spherically symmetric in the L system, the vector flux or the angular-space distribution of neutrons is obtained in a form of an infinite series of the spherical Bessel functions, from which the scalar flux and the net current are easily derived. This gives

EUR 479.e

NEUTRON DISTRIBUTION IN A CRITICAL SLAB BY THE MULTIPLE COLLISION METHOD by T. ASAOKA (EURATOM) and Y. NAKAHARA, K. SAITO (Japan Atomic Energy Research Institute, Tokai-mura, Ibaraki-ken, Japan)

European Atomic Energy Community — EURATOM
Joint Nuclear Research Center — Ispra Establishment (Italy)
Reactor Physics Department — Applied Mathematical Physics
Brussels, December 1963 — pages 47 — figures 8

The detailed distribution of monoenergetic neutrons, in a critical slab with finite thickness, is dealt with analytically by the multiple collision method or the random walk approach.

Under the assumption that the scattering of neutrons is spherically symmetric in the L system, the vector flux or the angular-space distribution of neutrons is obtained in a form of an infinite series of the spherical Bessel functions, from which the scalar flux and the net current are easily derived. This gives

EUR 479.e

NEUTRON DISTRIBUTION IN A CRITICAL SLAB BY THE MULTIPLE COLLISION METHOD by T. ASAOKA (EURATOM) and Y. NAKAHARA, K. SAITO (Japan Atomic Energy Research Institute, Tokai-mura, Ibaraki-ken, Japan)

European Atomic Energy Community — EURATOM
Joint Nuclear Research Center — Ispra Establishment (Italy)
Reactor Physics Department — Applied Mathematical Physics
Brussels, December 1963 — pages 47 — figures 8

The detailed distribution of monoenergetic neutrons, in a critical slab with finite thickness, is dealt with analytically by the multiple collision method or the random walk approach.

Under the assumption that the scattering of neutrons is spherically symmetric in the L system, the vector flux or the angular-space distribution of neutrons is obtained in a form of an infinite series of the spherical Bessel functions, from which the scalar flux and the net current are easily derived. This gives

definitely the discontinuity of the angular distribution at the boundary of the slab. Further, this infinite series converges fast and hence the accurate result can be obtained readily by truncating the sum at the first few terms, especially for the thinner slabs.

In the course of the formulation, the critical condition is also derived and shows that it coincides with the one obtained in the previous work. Finally, the numerical examples are given and discussed.

In Appendixes, it is shown how to correspond our formulation to the usual transport equation. According to this correspondence, for a bare sphere, the critical condition and the scalar flux are derived in similar forms to those for the slab, respectively. And the value of C, the mean number of secondaries per collision, is given within an error less than 0.01 % for every critical sphere whether the radius is large or small.

definitely the discontinuity of the angular distribution at the boundary of the slab. Further, this infinite series converges fast and hence the accurate result can be obtained readily by truncating the sum at the first few terms, especially for the thinner slabs.

In the course of the formulation, the critical condition is also derived and shows that it coincides with the one obtained in the previous work. Finally, the numerical examples are given and discussed.

In Appendixes, it is shown how to correspond our formulation to the usual transport equation. According to this correspondence, for a bare sphere, the critical condition and the scalar flux are derived in similar forms to those for the slab, respectively. And the value of C, the mean number of secondaries per collision, is given within an error less than 0.01 % for every critical sphere whether the radius is large or small.

definitely the discontinuity of the angular distribution at the boundary of the slab. Further, this infinite series converges fast and hence the accurate result can be obtained readily by truncating the sum at the first few terms, especially for the thinner slabs.

In the course of the formulation, the critical condition is also derived and shows that it coincides with the one obtained in the previous work. Finally, the numerical examples are given and discussed.

In Appendixes, it is shown how to correspond our formulation to the usual transport equation. According to this correspondence, for a bare sphere, the critical condition and the scalar flux are derived in similar forms to those for the slab, respectively. And the value of C, the mean number of secondaries per collision, is given within an error less than 0.01 % for every critical sphere whether the radius is large or small.

EUR 479.e

EUROPEAN ATOMIC ENERGY COMMUNITY - EURATOM

NEUTRON DISTRIBUTION IN A CRITICAL SLAB BY THE MULTIPLE COLLISION METHOD

by

T. ASAOKA (EURATOM) and
Y. NAKAHARA, K. SAITO
(Japan Atomic Energy Research Institute,
Tokai-mura, Ibaraki-ken, Japan)

1963

Joint Nuclear Research Center
Ispra Establishment - Italy

Reactor Physics Department
Applied Mathematical Physics

CONTENTS

NEUTRON DISTRIBUTION IN A CRITICAL SLAB BY THE MULTIPLE COLLISION METHOD

SUMMARY

The detailed distribution of monoenergetic neutrons, in a critical slab with finite thickness, is dealt with analytically by the multiple collision method or the random walk approach.

Under the assumption that the scattering of neutrons is spherically symmetric in the L system, the vector flux or the angular-space distribution of neutrons is obtained in a form of an infinite series of the spherical Bessel functions, from which the scalar flux and the net current are easily derived. This gives definitely the discontinuity of the angular distribution at the boundary of the slab. Further, this infinite series converges fast and hence the accurate result can be obtained readily by truncating the sum at the first few terms, especially for the thinner slabs.

In the course of the formulation, the critical condition is also derived and shows that it coincides with the one obtained in the previous work. Finally, the numerical examples are given and discussed.

In Appendixes, it is shown how to correspond our formulation to the usual transport equation. According to this correspondence, for a bare sphere, the critical condition and the scalar flux are derived in similar forms to those for the slab, respectively. And the value of c , the mean number of secondaries per collision, is given within an error less than 0.01% for every critical sphere whether the radius is large or small.

1. Introduction

The neutron transport problems have been generally treated according to the Boltzmann equation. In spite of much recent progress, however, only the simplest problems can be dealt with analytically by means of this. Therefore, we are forced to depend on the elementary diffusion theory or the numerical method relying on high-speed digital computers.

The multiple collision method is an effective analytical method, which is based on a viewpoint different from that of the Boltzmann equation, that is, the life-cycle viewpoint in contrast to the neutron-balance one.

By using this method, the one-group critical condition has already been derived accurately in a concise form, for a homogeneous slab in which the scattering of neutrons is spherically symmetric in the L system (Asaoka, 1961). It has been also shown that the two-group critical condition for the same system can be obtained analytically under some assumptions on the slowing down process. Furthermore, the reflection and the transmission of neutrons for the slab have been treated by this technique, and the accurate and plentiful informations about the neutron behaviour have been easily obtained (Asaoka, 1963).

The present work is concerned with a further development of the multiple collision method for obtaining the detailed distribution of neutrons in a critical slab. In the text, the formulation is made by following the elementary processes of the neutron statistically in order of its spatial movement. This formulation is compared with another one in Appendix 1, where the elementary processes are followed in order of time. In Appendix 2, it is shown how to correspond the present formulations to the transport equation expressing the conservation of neutrons. From this correspondence, the critical condition and the flux distribution for a bare sphere are obtained in Appendix 3.

2. Formulation

The discussion will be concerned with monoenergetic neutrons in an infinite homogeneous slab of finite thickness a in which scattering is spherically symmetric in the L system, as in the previous work upon the one-group critical condition.

In this previous work, the elementary processes of the neutron were followed statistically in order of time and then the critical condition was derived from the convergence of the total number of neutrons in the system as time proceeds indefinitely. Here, the elementary processes will be followed statistically in order of the spatial movement, as in the previous work on the reflection and transmission of neutrons, because this is an easier way to deal with the present problem (see Appendix 1).

Let x be the space coordinate, μ the directional cosine of the neutron velocity, Σ the macroscopic total cross section and c the mean number of secondary neutrons per collision.

Now consider an incident neutron with a directional cosine μ_1 , upon the surface of the slab at $x = 0$. It will travel for a certain distance r_1 in the direction with $\mu=\mu_1$ before it collides with a nucleus. The probability that neutrons will travel for a distance r_1 without collision is $e^{-\Sigma r_1}$ and the collision probability in dr_1 at r_1 is Σdr_1 . Hence, as a result of the first collision of the neutron, the number of neutrons with directional cosines between μ_2 and $\mu_2+d\mu_2$ will be $(c\Sigma/2)e^{-\Sigma r_1}dr_1 d\mu_2$. They will then travel for a certain distance r_2 in the direction μ_2 until they meet another nuclei . As a result of this second collision, the number of neutrons in $d\mu_3$ at μ_3 will amount to $(c\Sigma/2)^2 e^{-\Sigma(r_1+r_2)}dr_1 dr_2 d\mu_2 d\mu_3$ This process of movement will continue until the neutrons leak out of the slab.

Thus the number of neutrons having travelled for a distance r in the directions between μ and $\mu+d\mu$ as a result of the N-th collision after following a typical path shown in Fig. 1, is given by

$$\left(\frac{c\Sigma}{2}\right)^N exp[-\Sigma(r_1+r_2+\cdots+r_N+r)]\,dr_1\cdots dr_N\,d\mu_2\cdots d\mu_N\,d\mu, \quad N\geq 1. \tag{1}$$

Before performing integrations over all allowable paths for obtaining the number of neutrons travelling in the direction μ which cross an area normal to this direction at x , that is, the vector flux at x which comes from the neutrons having undergone the N-th collision, we must take into account some restrictions imposed upon the range of integration variables. First of all, in order to exclude the neutrons which have left the slab after the $(j-1)$- th collision, the following restrictions must be imposed :

$$0<\sum_{k=1}^{j} r_k\mu_k< a, \quad j=1,2,\cdots,N. \tag{2}$$

Besides these, another condition must be taken into consideration to get the vector flux at x . This reads as follows :

$$\sum_{j=1}^{N} r_j\mu_j+r\mu=x. \tag{3}$$

This condition is rewritten in a form of the Fourier representation of the Dirac delta function :

$$\delta\left(\sum_{j=1}^{N} r_j\mu_j + r\mu - x\right) = \frac{1}{2\pi}\int_{-\infty}^{\infty} d\rho \, \exp\left[i\rho\left(\sum_{j=1}^{N} r_j\mu_j + r\mu - x\right)\right], \tag{4}$$

and the conditions (2) are taken into account through Dirichlet's discontinuity factors :

$$\frac{1}{\pi}\int_{-\infty}^{\infty} dx_j \frac{\sin x_j}{x_j} e^{i x_j z_j} = \begin{cases} 1, & \text{when} \quad |z_j| < 1, \\ 0, & \text{when} \quad |z_j| > 1, \end{cases} \qquad j = 1, 2, \cdots, N.$$

Introducing these conditions into Eq. (1), replacing x_j by $y_j = \frac{2}{\Sigma a}\sum_{k=j}^{N+1} x_k$ where x_{N+1} stands for $(a/2)\rho$, and performing the integrations over all values of μ_j ($j = 2, \cdots, N$) , r_j ($j = 1, \cdots, N$) and r , as in the previous work (Asaoka, 1963), the vector flux at x coming from the neutrons undergone the N-th collision, is obtained as follows:

$$\phi_N(x, \mu; \mu_1) = \frac{1}{2\pi}\int_{-\infty}^{\infty} dy \frac{\exp[-i\Sigma(x - a/2)y]}{1 - i\mu y} G_{N+1}(y; \mu_1), \tag{5}$$

where the independent variable y_{N+1} is replaced by y . The functions $G_{j+1}(y;\mu_1)$'s are expanded in the spherical Bessel functions :

$$G_{j+1}(y;\mu_1) = \sum_{m=0}^{\infty} b_m^{j+1}(\mu_1) j_m\left(\frac{\Sigma a}{2} y\right), \quad j = 1, \cdots, N, \tag{6}$$

of which the coefficients $b_m^{j+1}(\mu_1)$'s are to be determined by the following recurrence relation derived by using the Gegenbauer's addition theorem, $j_0(y-z) = \sum_{n=0}^{\infty}(2n+1) j_n(y) j_n(z)$, and the orthogonality relation for the spherical Bessel functions :

$$\left.\begin{aligned} &\frac{1}{(2n+1)c}\, b_n^{\,j+1}(\mu_1)=\sum_{\substack{m=0\\ n+m=\text{even}}}^{\infty} b_m^{\,j}(\mu_1)\, J(n,m)\,, \qquad j=N,N-1,\cdots,2,\\ &b_n^{\,2}(\mu_1)=(2n+1)\frac{c\Sigma a}{2\mu_1}\, j_n\!\left(-i\frac{\Sigma a}{2\mu_1}\right)\exp\!\left(-\frac{\Sigma a}{2\mu_1}\right), \end{aligned}\right\} \tag{7}$$

where

$$J(n,m)=\frac{\Sigma a}{\pi}\int_0^{\infty} dy\, j_n\!\left(\frac{\Sigma a}{2}y\right) j_m\!\left(\frac{\Sigma a}{2}y\right)\frac{\tan^{-1} y}{y} \tag{8}$$

of which the concrete expressions have been shown in the previous report (Asaoka, 1963).

For a critical system, this component of the vector flux, $\Phi_N(x,\mu;\mu_1)$, should tend to a constant value independently of N as the value of N proceeds indefinitely. In other words, the value of $b_m^{N+1}(\mu_1)$ should tend to a constant one, $b_m(\mu_1)$, as seen from Eqs. (5) and (6). The equation by which these values of $b_m(\mu_1)$' s are to be determined, is easily obtained from Eq. (7) :

$$\frac{1}{(2n+1)c}\, b_n(\mu_1)=\sum_{\substack{m=0\\ n+m=\text{even}}}^{\infty} b_m(\mu_1)\, J(n,m)\,, \quad n=0,1,2,\cdots . \tag{9}$$

According to this infinite set of linear equations, it is seen that the values of $b_m(\mu_1)$'s are independent of the value of μ_1 , as expected, and hence hereafter we will use the notation b_m instead of $b_m(\mu_1)$. And further, b_{2n}' s and b_{2n+1}' s are independent of each other because the former are coupled only with one another but not with the latter, and vice versa. Thus the condition that Eq. (9) should have a nontrivial solution is that the determinant of the coefficients shall vanish :

$$\left|\frac{\delta_{nm}}{(2n+1)c}-J(n,m)\right|=0, \quad n,m=0,2,4,\cdots \text{ or } 1,3,5,\cdots . \tag{10}$$

This characteristic equation with even values for both n and m is nothing but the one-group critical condition that was derived in the previous work (Asaoka, 1961). The other equation with odd values for both n and m does not give the smallest eigenvalue c as easily seen numerically (see the discussion following Eq. (A.35) in Appendix 3) and hence the value of the determinant must differ from zero for the critical system. It is thus seen that all values of b_{2n+1}'s are identically zero. And the ratios among the values of b_{2n}'s are given as follows:

$$b_0 : b_2 : b_4 : \cdots\cdots$$

$$= \begin{vmatrix} -J(0,2) & -J(0,4) & -J(0,6) \cdots \\ 1/5c - J(2,2) & -J(2,4) & -J(2,6) \\ -J(4,2) & 1/9c - J(4,4) & -J(4,6) \\ \vdots & & \end{vmatrix} : \begin{vmatrix} -1/c + J(0,0) & -J(0,4) \cdots \\ J(2,0) & -J(2,4) \\ J(4,0) & 1/9c - J(4,4) \\ \vdots & \end{vmatrix} : \begin{vmatrix} -J(0,2) & -1/c + J(0,0) & -J(0,6) \cdots \\ 1/5c - J(2,2) & J(2,0) & -J(2,6) \\ -J(4,2) & J(4,0) & -J(4,6) \\ \vdots & & \end{vmatrix} : \cdots\cdots . \tag{11}$$

The vector flux in the critical system is thus written in the following form according to Eqs. (5) and (6) :

$$\phi(x,\mu) = \frac{1}{2\pi} \sum_{n=0}^{\infty} b_{2n} \int_{-\infty}^{\infty} dy \, \frac{\exp[-i\Sigma(x-a/2)y]}{1-i\mu y} \, j_{2n}\left(\frac{\Sigma a}{2} y\right). \tag{12}$$

From this, it is easily seen that

$$\phi(x,\mu) = \phi(a-x,-\mu), \tag{13}$$

$$\phi(0,\mu) = 0, \quad \mu > 0, \tag{14}$$

because, in the case of $x = 0$, the integrand has only one pole at $y = -i/\mu$ in the half-plane below the real axis and besides we can take the path of integration in the upper half-plane. The integration in Eq. (12) can be easily performed to give :

$$\phi(x,\mu)=\sum_{n=0}^{\infty} b_{2n}\Big[\tfrac{i}{2}\mathcal{R}\Big(\frac{e^{i\Sigma(a-x)y}}{1-i\mu y}j_{2n}^{1}(\tfrac{\Sigma a}{2}y)\Big)_{y=0}-\tfrac{i}{2}\mathcal{R}\Big(\frac{e^{-i\Sigma x y}}{1-i\mu y}j_{2n}^{2}(\tfrac{\Sigma a}{2}y)\Big)_{y=0}$$

$$+\frac{1}{\mu}j_{2n}^{2}(-i\tfrac{\Sigma a}{2\mu})e^{-\Sigma x/\mu}\Big],\qquad \mu>0, \tag{15}$$

where

$$j_{2n}(z)=j_{2n}^{1}(z)e^{iz}+j_{2n}^{2}(z)e^{-iz}\quad\big(j_{2n}^{1}(z)=j_{2n}^{2}(-z)\big)$$

and $\mathcal{R}(f(y))_{y=0}$ stands for the residue of $f(y)$ at $y=0$.

The total or scalar flux is then obtained in the form from Eq. (12) :

$$\phi(x)=\int_{-1}^{1}d\mu\,\phi(x,\mu)=\frac{1}{\pi}\sum_{n=0}^{\infty}b_{2n}\int_{-\infty}^{\infty}dy\,\exp[-i\Sigma(x-a/2)y]\frac{\tan^{-1}y}{y}j_{2n}(\tfrac{\Sigma a}{2}y), \tag{16}$$

from which it is easily seen that $\phi(x)=\phi(a-x)$. Performing the integration, this gives :

$$\phi(x)=\sum_{n=0}^{\infty}b_{2n}\Big[i\mathcal{R}\Big(\frac{\tan^{-1}y}{y}j_{2n}^{1}(\tfrac{\Sigma a}{2}y)e^{i\Sigma(a-x)y}\Big)_{y=0}-i\mathcal{R}\Big(\frac{\tan^{-1}y}{y}j_{2n}^{2}(\tfrac{\Sigma a}{2}y)e^{-i\Sigma x y}\Big)_{y=0}$$

$$+\int_{1}^{\infty}\frac{dt}{t}j_{2n}^{1}(i\tfrac{\Sigma a}{2}t)e^{-\Sigma(a-x)t}+\int_{1}^{\infty}\frac{dt}{t}j_{2n}^{2}(-i\tfrac{\Sigma a}{2}t)e^{-\Sigma x t}\Big]$$

$$=\sum_{n=0}^{\infty}b_{2n}\Big\{i\mathcal{R}\Big[\frac{\tan^{-1}y}{y}j_{2n}^{1}(\tfrac{\Sigma a}{2}y)\big(e^{i\Sigma(a-x)y}+e^{i\Sigma x y}\big)\Big]_{y=0}+\int_{1}^{\infty}\frac{dt}{t}j_{2n}^{1}(i\tfrac{\Sigma a}{2}t)\big(e^{-\Sigma(a-x)t}+e^{-\Sigma x t}\big)\Big\}. \tag{17}$$

This is composed of two parts, as well known; the asymptotic one resulting from the pole $y=0$ and the transient one from the cuts along the imaginary axis from $y=i$ to $y=i\infty$ and from $y=-i$ to $y=-i\infty$.

Moreover, the net current is given as follows :

$$J(x)=\int_{-1}^{1}d\mu\,\mu\,\phi(x,\mu)=\frac{i}{\pi}\sum_{n=0}^{\infty}b_{2n}\int_{-\infty}^{\infty}\frac{dy}{y}\Big(1-\frac{\tan^{-1}y}{y}\Big)j_{2n}(\tfrac{\Sigma a}{2}y)e^{-i\Sigma(x-a/2)y}, \tag{18}$$

from which the well-known relation, $J(x)=-J(a-x)$, is easily seen. This becomes :

$$J(x)=\sum_{n=0}^{\infty} b_{2n}\left\{\Re\left[\frac{1}{y}\left(1-\frac{\tan^{-1}y}{y}\right)j_{2n}'\left(\frac{\Sigma a}{2}y\right)\left(e^{i\Sigma xy}-e^{i\Sigma(a-x)y}\right)\right]_{y=0}\right.$$

$$\left.+\int_1^{\infty}\frac{dt}{t^2}j_{2n}'\left(i\frac{\Sigma a}{2}t\right)\left(e^{-\Sigma xt}-e^{-\Sigma(a-x)t}\right)\right\}. \tag{19}$$

3. Results and Discussions

The vector flux, the scalar flux and the net current have been written in forms of an infinite series, respectively, and hence we are forced to truncate the sum for obtaining the numerical results. That is, neglecting all terms beyond $j_M(\frac{\Sigma a}{2}y)$ on the right side of Eq. (6), the coefficients b_{2n}'s ($2n \leq M$) are determined approximately. We shall call this approximation the " j_M-approximation", as in the previous work (Asaoka, 1963). The results in the j_{2N+1}-approximation are the same as those in the j_{2N}-approximation for the present problem. The ratios among b_{2n}'s in the j_2- and j_4- approximation are given in the following forms, respectively, according to Eq. (11) and the critical condition :

(a) The j_2- approximation;

$$\frac{b_2}{b_0}=\frac{1/c-J(0,0)}{J(0,2)}=\frac{J(0,2)}{1/(5c)-J(2,2)}, \tag{20}$$

(b) The j_4- approximation;

$$\frac{b_2}{b_0}=\frac{J(0,2)J(0,4)+J(2,4)(1/c-J(0,0))}{J(0,2)J(2,4)+J(0,4)(1/(5c)-J(2,2))},$$

$$\frac{b_4}{b_0}=\frac{(1/c-J(0,0))(1/(5c)-J(2,2))-(J(0,2))^2}{J(0,2)J(2,4)+J(0,4)(1/(5c)-J(2,2))}=\frac{J(0,4)+J(2,4)b_2/b_0}{1/(7c)-J(4,4)}. \tag{21}$$

The value of c , the mean number of secondaries per collision, required to keep the slab of thickness $\Sigma a = 2\alpha$ to be critical, has been already obtained by solving the critical equation, Eq. (10) with even values for both n and m (Asaoka, 1961). These values for small α and for large α have been given in the forms, respectively (γ is the Euler-Mascheroni constant) :

(a) The $\dot{j}_0$ -approximation;

$$\frac{1}{c} \sim -\left(1-\frac{3/2-\gamma}{\ln 2\alpha}\right)\alpha \ln 2\alpha \quad \text{and} \quad 1-\frac{1}{4\alpha} ,$$

(b) The $\dot{j}_2$ -approximation;

$$\frac{1}{c} \sim -\left(1-\frac{3/2-\gamma}{\ln 2\alpha}+\frac{5/144}{(\ln 2\alpha)^2}\right)\alpha \ln 2\alpha \qquad \text{and} \quad 1-\frac{5}{6\alpha^2}+\frac{565}{432\alpha^3}, \tag{22}$$

(c) The $\dot{j}_4$-approximation;

$$\frac{1}{c} \sim -\left(1-\frac{3/2-\gamma}{\ln 2\alpha}+\frac{7/200}{(\ln 2\alpha)^2}\right)\alpha \ln 2\alpha \qquad \text{and} \quad 1-\frac{11-\sqrt{133}}{3\alpha^2}+\frac{281541-23035\sqrt{133}}{20520\alpha^3}$$

The leading terms of Eqs. (20) and (21) for small α are thus given by

(a) The $\dot{j}_2$ -approximation;

$$\frac{f_2}{f_0} \sim -\frac{5/12}{\ln 2\alpha}\left(1+\frac{13/12-\gamma}{\ln 2\alpha}+\frac{41/36-13\gamma/6+\gamma^2}{(\ln 2\alpha)^2}\right), \tag{23}$$

(b) The $\dot{j}_4$ -approximation;

$$\left.\begin{aligned} \frac{f_2}{f_0} &\sim -\frac{5/12}{\ln 2\alpha}\left(1+\frac{131/120-\gamma}{\ln 2\alpha}+\frac{2759/2400-131\gamma/60+\gamma^2}{(\ln 2\alpha)^2}\right), \\ \frac{f_4}{f_0} &\sim \frac{1/20}{\ln 2\alpha}\left(1+\frac{139/60-\gamma}{\ln 2\alpha}+\frac{11681/2880-139\gamma/30+\gamma^2}{(\ln 2\alpha)^2}\right). \end{aligned}\right\} \tag{24}$$

On the other hand, for large values of α ,

(a) The $\dot{j}_2$ -approximation;

$$\frac{f_2}{f_0} \sim 1-\frac{4}{3\alpha} , \tag{25}$$

(b) The j_4-approximation;

$$\left.\begin{aligned} \frac{b_2}{b_0} &\sim \frac{5}{21}(\sqrt{133}-7)\left(1-\frac{2335\sqrt{133}-1387}{13680\alpha}\right), \\ \frac{b_4}{b_0} &\sim \frac{5}{21}\left(\sqrt{133}-\frac{56}{5}\right)\left(1-73\frac{19+2\sqrt{133}}{6840\alpha}\right). \end{aligned}\right\} \tag{26}$$

The vector flux (15), the scalar flux (17) and the net current (19) up to in the j_4-approximation are written in the following forms, respectively :

$$\begin{aligned} \frac{2\alpha}{b_0}\phi(\xi,\mu) = {} & 1-e^{-\xi/\mu}-\left[1-3\frac{\xi}{\alpha}\left(1-\frac{\xi}{2\alpha}\right)+\frac{3\mu}{\alpha}\left(1-\frac{\xi}{\alpha}\right)+\frac{3\mu^2}{\alpha^2}-\left(1+\frac{3\mu}{\alpha}+\frac{3\mu^2}{\alpha^2}\right)e^{-\xi/\mu}\right]\frac{b_2}{b_0} \\ & +\Big[1-10\frac{\xi}{\alpha}\left(1-\frac{\xi}{2\alpha}\right)+\frac{35}{2}\left(\frac{\xi}{\alpha}\right)^2\left(1-\frac{\xi}{2\alpha}\right)^2+\frac{35\mu}{2\alpha}\left(1-\frac{\xi}{\alpha}\right)\left(\left(1-\frac{\xi}{\alpha}\right)^2-\frac{3}{7}\right)+45\frac{\mu^2}{\alpha^2}\left(1-\frac{7}{3}\frac{\xi}{\alpha}\left(1-\frac{\xi}{2\alpha}\right)\right) \\ & +105\frac{\mu^3}{\alpha^3}\left(1-\frac{\xi}{\alpha}\right)+105\frac{\mu^4}{\alpha^4}-\left(1+10\frac{\mu}{\alpha}+45\frac{\mu^2}{\alpha^2}+105\frac{\mu^3}{\alpha^3}+105\frac{\mu^4}{\alpha^4}\right)e^{-\xi/\mu}\Big]\frac{b_4}{b_0}, \quad \mu>0, \end{aligned} \tag{27}$$

$$\begin{aligned} \frac{2\alpha}{b_0}\phi(\xi) = {} & 2-E_2-\left[2-6\frac{\xi}{\alpha}\left(1-\frac{\xi}{2\alpha}\right)+\frac{2}{\alpha^2}-E_2-\frac{3}{\alpha}E_3-\frac{3}{\alpha^2}E_4\right]\frac{b_2}{b_0} \\ & +\Big[2-20\frac{\xi}{\alpha}\left(1-\frac{\xi}{2\alpha}\right)+35\left(\frac{\xi}{\alpha}\right)^2\left(1-\frac{\xi}{2\alpha}\right)^2+\frac{30}{\alpha^2}\left(1-\frac{7}{3}\frac{\xi}{\alpha}\left(1-\frac{\xi}{2\alpha}\right)\right)+\frac{42}{\alpha^4} \\ & -E_2-\frac{10}{\alpha}E_3-\frac{45}{\alpha^2}E_4-\frac{105}{\alpha^3}E_5-\frac{105}{\alpha^4}E_6\Big]\frac{b_4}{b_0}, \end{aligned} \tag{28}$$

$$\begin{aligned} \frac{2\alpha}{b_0}J(\xi) = {} & E_3'-\left[\frac{2}{\alpha}\left(1-\frac{\xi}{\alpha}\right)+E_3'+\frac{3}{\alpha}E_4'+\frac{3}{\alpha^2}E_5'\right]\frac{b_2}{b_0}+\Big[\frac{35}{3\alpha}\left(1-\frac{\xi}{\alpha}\right)\left(\left(1-\frac{\xi}{\alpha}\right)^2-\frac{3}{7}\right) \\ & +\frac{42}{\alpha^3}\left(1-\frac{\xi}{\alpha}\right)+E_3'+\frac{10}{\alpha}E_4'+\frac{45}{\alpha^2}E_5'+\frac{105}{\alpha^3}E_6'+\frac{105}{\alpha^4}E_7'\Big]\frac{b_4}{b_0}, \end{aligned} \tag{29}$$

where $\alpha=\Sigma a/2$, $\xi=\Sigma x$, $E_n=E_n(2\alpha-\xi)+E_n(\xi)$, $E_n'=E_n(2\alpha-\xi)-E_n(\xi)$ and

$$E_n(y)=\int_1^\infty dt\, e^{-yt}t^{-n}.$$

As a special case, the vector flux for $\mu<0$ at the boundary of the slab is given in the form according to Eqs. (13) and (27) :

$$\begin{aligned} \frac{2\alpha}{b_0}\phi(0,\mu) = {} & 1-e^{2\alpha/\mu}-\left[1+\frac{3\mu}{\alpha}+\frac{3\mu^2}{\alpha^2}-\left(1-\frac{3\mu}{\alpha}+\frac{3\mu^2}{\alpha^2}\right)e^{2\alpha/\mu}\right]\frac{b_2}{b_0} \\ & +\left[1+10\frac{\mu}{\alpha}+45\frac{\mu^2}{\alpha^2}+105\frac{\mu^3}{\alpha^3}+105\frac{\mu^4}{\alpha^4}-\left(1-10\frac{\mu}{\alpha}+45\frac{\mu^2}{\alpha^2}-105\frac{\mu^3}{\alpha^3}+105\frac{\mu^4}{\alpha^4}\right)e^{2\alpha/\mu}\right]\frac{b_4}{b_0}, \\ & \mu<0. \end{aligned} \tag{30}$$

Upon substituting Eq. (23) or (24) into Eqs. (27), (28) and (29), respectively, we get the leading terms for small α/μ as follows :

(a) The j_0-approximation;

$$\left.\begin{aligned}
&\frac{2\alpha}{f_0}\phi(\xi,\mu)\sim\frac{\xi}{\mu}\left(1-\frac{\xi}{2\mu}\right),\quad \mu>0,\\
&\frac{2\alpha}{f_0}\phi(\xi)\sim 2\alpha\left\{-\left(1-\frac{\xi}{2\alpha}\right)\ln(2\alpha-\xi)-\frac{\xi}{2\alpha}\ln\xi+1-\gamma\right\},\\
&\frac{2\alpha}{f_0}J(\xi)\sim -2\alpha\left\{1-\frac{\xi}{\alpha}+\frac{(2\alpha-\xi)^2}{4\alpha}\ln(2\alpha-\xi)-\frac{\xi^2}{4\alpha}\ln\xi\right\},
\end{aligned}\right\}\tag{31}$$

(b) The j_2-approximation;

$$\left.\begin{aligned}
&\frac{2\alpha}{f_0}\phi(\xi,\mu)\sim\frac{\xi}{\mu}\left\{1-\frac{\xi}{2\mu}+\left(1-\frac{\xi}{\alpha}\right)\left(1-\frac{\xi}{2\alpha}\right)\frac{5/12}{\ln 2\alpha}\right\},\quad \mu>0,\\
&\frac{2\alpha}{f_0}\phi(\xi)\sim 2\alpha\left\{-\left(1-\frac{\xi}{2\alpha}\right)\ln(2\alpha-\xi)-\frac{\xi}{2\alpha}\ln\xi+1-\gamma\right.\\
&\qquad\qquad\left.+\frac{\xi}{2\alpha}\left(1-\frac{\xi}{\alpha}\right)\left(1-\frac{\xi}{2\alpha}\right)\ln\left(\frac{2\alpha}{\xi}-1\right)\frac{5/12}{\ln 2\alpha}\right\},\\
&\frac{2\alpha}{f_0}J(\xi)\sim -2\alpha\left\{1-\frac{\xi}{\alpha}+\frac{(2\alpha-\xi)^2}{4\alpha}\ln(2\alpha-\xi)-\frac{\xi^2}{4\alpha}\ln\xi-\frac{\xi}{\alpha}\left(1-\frac{\xi}{\alpha}\right)\left(1-\frac{\xi}{2\alpha}\right)\frac{5/12}{\ln 2\alpha}\right\},
\end{aligned}\right\}\tag{32}$$

(c) The j_4-approximation;

$$\left.\begin{aligned}
&\frac{2\alpha}{f_0}\phi(\xi,\mu)\sim\frac{\xi}{\mu}\left\{1-\frac{\xi}{2\mu}+\left(1-\frac{\xi}{\alpha}\right)\left(1-\frac{\xi}{2\alpha}\right)\left(1-\frac{3}{8}\frac{\xi}{\alpha}+\frac{3}{16}\frac{\xi^2}{\alpha^2}\right)\frac{7/15}{\ln 2\alpha}\right\},\quad \mu>0,\\
&\frac{2\alpha}{f_0}\phi(\xi)\sim 2\alpha\left\{-\left(1-\frac{\xi}{2\alpha}\right)\ln(2\alpha-\xi)-\frac{\xi}{2\alpha}\ln\xi+1-\gamma\right.\\
&\qquad\qquad\left.+\frac{\xi}{2\alpha}\left(1-\frac{\xi}{\alpha}\right)\left(1-\frac{\xi}{2\alpha}\right)\left(1-\frac{3}{8}\frac{\xi}{\alpha}+\frac{3}{16}\frac{\xi^2}{\alpha^2}\right)\ln\left(\frac{2\alpha}{\xi}-1\right)\frac{7/15}{\ln 2\alpha}\right\},\\
&\frac{2\alpha}{f_0}J(\xi)\sim -2\alpha\left\{1-\frac{\xi}{\alpha}+\frac{(2\alpha-\xi)^2}{4\alpha}\ln(2\alpha-\xi)-\frac{\xi^2}{4\alpha}\ln\xi\right.\\
&\qquad\qquad\left.-\frac{\xi}{\alpha}\left(1-\frac{\xi}{\alpha}\right)\left(1-\frac{\xi}{2\alpha}\right)\left(1-\frac{3}{8}\frac{\xi}{\alpha}+\frac{3}{16}\frac{\xi^2}{\alpha^2}\right)\frac{7/15}{\ln 2\alpha}\right\},
\end{aligned}\right\}\tag{33}$$

and the leading terms of $\frac{2\alpha}{f_0}\phi(\xi,\mu)$ for $\mu<0$ are obtained immediately according to Eq. (13) by replacing ξ and μ by $2\alpha-\xi$ and $-\mu$, respectively, in the first equation in Eq. (31), (32) or (33).

For large α , Eq. (27), (28) or (29) gives the following expressions according to Eq. (25) or (26) :

(a) The j_0 -approximation;

$$
\left.\begin{aligned}
&\frac{2\alpha}{b_0}\phi(0,\mu)\sim 1\ ,\quad \mu<0\\
&\frac{2\alpha}{b_0}\phi(\alpha,\mu)\sim 1,\\
&\frac{2\alpha}{b_0}\phi(\xi)\sim 1-\xi(\ln\xi+\gamma-1),\qquad \xi\ll 1,\\
&\frac{2\alpha}{b_0}J(\xi)\sim -\frac{1}{2}(1-2\xi),\qquad \xi\ll 1,
\end{aligned}\right\}\qquad (34)
$$

(b) The j_2 -approximation;

$$
\left.\begin{aligned}
&\frac{2\alpha}{b_0}\phi(0,\mu)\sim \frac{4}{3\alpha}\left(1-\frac{9}{4}\mu\right),\quad \mu<0,\\
&\frac{2\alpha}{b_0}\phi(\alpha,\mu)\sim \frac{3}{2}\left(1-\frac{4}{9\alpha}\right),\\
&\frac{2\alpha}{b_0}\phi(\xi)\sim \frac{17}{6\alpha}\left\{1-\frac{8}{17}\xi\left(\ln\xi+\gamma-\frac{13}{4}\right)\right\},\quad \xi\ll 1,\\
&\frac{2\alpha}{b_0}J(\xi)\sim -\frac{5}{3\alpha}\left(1+\frac{1}{10}\xi\right),\quad \xi\ll 1,
\end{aligned}\right\}\qquad (35)
$$

(c) The j_4 -approximation;

$$
\left.\begin{aligned}
&\frac{2\alpha}{b_0}\phi(0,\mu)\sim \frac{38-2\sqrt{133}}{9\alpha}\left(1-15\,\frac{19-\sqrt{133}}{76}\mu\right),\quad \mu<0,\\
&\frac{2\alpha}{b_0}\phi(\alpha,\mu)\sim \frac{5}{27}(\sqrt{133}-4)\left(1-\frac{1646\sqrt{133}-21261}{44460\alpha}\right),\\
&\frac{2\alpha}{b_0}\phi(\xi)\sim \frac{271-19\sqrt{133}}{18\alpha}\left\{1-\frac{874+30\sqrt{133}}{2119}\xi\left(\ln\xi+\gamma-\frac{361-15\sqrt{133}}{76}\right)\right\},\quad \xi\ll 1,\\
&\frac{2\alpha}{b_0}J(\xi)\sim -\frac{2}{3\alpha}(14-\sqrt{133})\left(1-\frac{5\sqrt{133}-29}{108}\xi\right),\quad \xi\ll 1.
\end{aligned}\right\}\qquad (36)
$$

As seen from Eqs. (31), (32) and (33), the results converge fast for thinner slabs as going to the higher order approximation and hence even the results in the j_0-approximation may give the accurate ones. On the other hand, the results for thicker slabs do not converge so fast but the ones in the j_4 -approximation may be regarded to be accurate, as seen from Eqs. (34), (35) and (36).

It may be worth while to review the results on the so-called extrapolation distance d, the distance between the boundary of the medium and the point at which the asymtotic neutron flux in a form of $\sin[B(x+d)]$ would go through zero. This has been given in the form (Asaoka, 1961):

$$\Sigma d = \frac{\pi/2}{\sqrt{3(1-1/c)}} - \alpha, \tag{37}$$

in accordance with the critical condition in the diffusion theory. Substituting the leading terms of $1/c$ for large α shown in Eq. (22) into Eq. (37), we have

(a) The j_2-approximation;

$$\Sigma d \sim \left(\frac{\pi}{\sqrt{10}} - 1\right)\alpha + \frac{\pi}{\sqrt{10}}\frac{113}{144}$$

$$\left(\frac{113}{144} = 0.78472\right),$$

(b) The j_4-approximation;

$$\Sigma d \sim \left(\frac{\pi/2}{\sqrt{14-\sqrt{133}}} - 1\right)\alpha + \frac{\pi/2}{\sqrt{14-\sqrt{133}}}\frac{15713-523\sqrt{133}}{13680}$$

$$\left(\frac{15713-523\sqrt{133}}{13680} = 0.70771\right). \tag{38}$$

As seen from these expressions, roughly speaking, π is replaced by $\sqrt{10}$ in the j_2-approximation and by $2\sqrt{14-\sqrt{133}} = 3.141616$ in the j_4-approximation.

The extrapolated end-point ξ_0, the distance beyond the boundary of the medium at which the asymptotic flux vanishes, is obtained from the following equation according to Eq. (17) together with Eq. (28):

$$1 - \left[1 + 3\frac{\xi_0}{\alpha}\left(1+\frac{\xi_0}{2\alpha}\right) + \frac{1}{\alpha^2}\right]\frac{b_2}{b_0}$$
$$+ \left[1 + 10\frac{\xi_0}{\alpha}\left(1+\frac{\xi_0}{2\alpha}\right) + \frac{35}{2}\left(\frac{\xi_0}{\alpha}\right)^2\left(1+\frac{\xi_0}{2\alpha}\right)^2 + \frac{15}{\alpha^2}\left(1+\frac{7}{3}\frac{\xi_0}{\alpha}\left(1+\frac{\xi_0}{2\alpha}\right)\right) + \frac{21}{\alpha^4}\right]\frac{b_4}{b_0} = 0. \tag{39}$$

For large α , this gives

$$\left.\begin{array}{l} \text{(a) The } j_2 \text{-approximation;} \\ \qquad \xi_0 \sim 4/9, \\ \\ \text{(b) The } j_4 \text{-approximation;} \\ \qquad \xi_0 \sim (19+\sqrt{133})/45 = 0.67850. \end{array}\right\} \qquad (40)$$

Moreover, the accuracy of the results for large α in the j_4 -approximation will be shown by comparing some results in Eq. (36) with the exact ones. The exact results for the infinite half-space with $c = 1$ has been given as follows (Case et al., 1953):

$$\phi(0,-1)/\phi(0,-0) = 2.9078,$$

$$\bar{\mu} = \int_{-1}^{0} d\mu\, \mu\, \phi(0,\mu) \Big/ \int_{-1}^{0} d\mu\, \phi(0,\mu) = -0.5774,$$

$$\phi(\xi) = \phi(0)[1 + \tfrac{1}{2}\xi \ln\tfrac{1}{\xi} + O(\xi)], \quad \xi \ll 1.$$

Our results corresponding to these are

$$\phi(0,-1)/\phi(0,-0) = 2.4738$$

$$\bar{\mu} = J(0)/\phi(0) = -\frac{1267-5\sqrt{133}}{2119} = -0.5707,$$

$$\phi(\xi) = \phi(0)[1 + 0.5757\, \xi \ln\tfrac{1}{\xi} + O(\xi)], \quad \xi \ll 1.$$

Even in the extreme case, for which our j_4-approximation becomes to be rather poor as mentioned already, it is shown that the coincidence of our results with the exact ones is not so bad, and hence it is believed that the j_4-approximation gives an accurate result for every system whether thin or thick.

Some numerical examples are shown in Figs. 2–5. In Fig. 2, $(2\alpha/\ell_0)\phi(\xi,\mu)$ in the slab with α=0.005 is shown for the values of ξ=0 and 0.005, that is, the vector flux at the boundary and at the center of the slab, respectively. As expected, the results in the j_0 -approximation differ only a little from those in the j_2 -approximation and the difference between the results in the j_2- and the j_4-approximation is hardly recognized in this figure. And it is seen, as a matter of course, that the vector flux at the center takes a sharper maximum at μ=0, the direction in parallel with the boundary, than that at the boundary.

Fig. 3 shows the vector flux for the values of ξ =0,0.1 and 0.5 in the slab with α=0.5. From this figure, it is seen how to be created the symmetric distribution at the center of the slab, from the unsymmetric one with a discontinuity at μ=0 at the boundary. The difference between the results in the j_2- and the j_4-approximation is scarcely recognized also in this figure.

In Fig. 4 are shown the results of the vector flux in the slab with α=10, for the values of ξ=0,1,4 and 10. Here it is seen much difference between the results in the j_0- and the j_2-approximation, especially for those at ξ=0, but a little difference between those in the j_2- and the j_4-approximation.

In the last figure, Fig. 5, are shown the results of the scalar flux within the slabs with α=0.005, 0.5 and 10, respectively. The value of it at the center of the slab is normalized to unity, and the results obtained by Inönü are also shown for comparison (Inönü, 1959). He calculated, by applying a variational method directly to an integral equation governing the balance of neutrons, the first-flight nonescape probability for the persisting neutron distribution within the slab. Since the inverse of this nonescape probability should be equal to the value of C required to keep the system to be critical, comparison of this value with our result has been made already in the previous work (Asaoka, 1961). This comparison has shown that these values coincide nearly completely with our results in the j_2-approximation and are slightly larger than those in the j_4-approximation.

Similarly, his persisting distribution obtained in a form of that $1-u_0(\alpha)(1-\xi/\alpha)^2$, coincides with our result in the j_2-approximation nearly completely as seen from Fig. 5. And it behaves slightly higher than that in the j_4-approximation near the boundary, as indicated by him, and slightly lower halfway between the center and the boundary, for the slabs with the smaller α . For the slabs with the larger values of α , on the contrary, his distribution behaves slightly higher than that in the j_4-approximation, halfway between the center and the boundary.

4. Conclusions

The detailed distribution of neutrons in the critical slab with finite thickness, has been obtained accurately in the random walk approach.

One of the questions remaining to be solved in the reactor theory is how to deal with the neutron transport in a finite system through a simple method, whether the system is large or small.

It may be believed that the multiple collision method is a way to solve this question. The essential point of this method lies in the introduction of the discontinuity factors, by which we can easily take into account the finiteness of the system and fix the observing point (see also Appendixes 2 and 3), as well as the adoption of a viewpoint different from the usual transport equation. As a result of this, the neutron transport problems for a finite system can be dealt with in a similar way as those for an infinite system. Further, it may be mentioned that the expansion in the spherical Bessel functions is a useful way to obtain the results easily.

Although our works so far have been performed under the assumption that the scattering of neutrons is spherically symmetric in the L system, the method will be extended to the case without this assumption, even with other geometries than the homogeneous slab (regarding a spherical geometry, see Appendix 3). Moreover. it is hoped to extend this technique to more general problems.

Acknowledgements —— The authors wish to thank Prof. R. Nozawa of Tokyo Institute of Technology and Dr. G. Blässer for discussions regarding this work.

References

Asaoka T. (1961) —— J. Atomic Energy Soc. Japan 3, 531.

Asaoka T. (1963) —— Reflection and Transmission of Neutrons by the Multiple Collision Method, EUR 367.e

Case K.M., Hoffmann F. and Placzek G. (1953) —— Introduction to the Theory of Neutron Diffusion, Vol. 1, Sec. 18.1.

Inönü E. (1959) —— Nuclear Sci. and Engineering 5, 248.

Appendix 1. Another Formulation

Here it will be shown another formulation for obtaining the vector flux, Eq. (12), where the elementary processes of the neutron are followed in order of time.

Now consider an ancestor neutron with a directional cosine μ_1 at $x=0$, for example, at time $t=0$; it will travel for a time t_1 in the direction with $\mu=\mu_1$ before it collides with a nucleus. Since this probability is $e^{-\Sigma v t_1}$, v being the constant speed of neutrons, and the collision probability in dt_1 at t_1 is $\Sigma v dt_1$, the number of neutrons with directional cosines between μ_2 and $\mu_2+d\mu_2$ as a result of this collision becomes to $(c\Sigma v/2)e^{-\Sigma v t_1}dt_1 d\mu_2$. They will then travel for a certain time t_2 in the direction μ_2 until they meet another nuclei. The number of neutrons in $d\mu_3$ at μ_3 after the second collision will amount to $(c\Sigma v/2)^2 e^{-\Sigma v(t_1+t_2)}dt_1 dt_2 d\mu_2 d\mu_3$.

Thus the number of neutrons with directional cosines between μ and $\mu+d\mu$ at time t as a result of the N-th collision after following a typical path shown in Fig. A.1, is given by

$$\left(\frac{c\Sigma v}{2}\right)^N e^{-\Sigma v t}\, dt_1\cdots dt_N\, d\mu_2\cdots d\mu_N\, d\mu, \quad N\geq 1. \tag{A.1}$$

In order to obtain the vector flux at x within the slab of finite thickness a , the following conditions must be taken into account:

$$\sum_{j=1}^{N} v\mu_j t_j + v\mu\left(t-\sum_{j=1}^{N} t_j\right) = x, \tag{A.2}$$

$$0 < \sum_{k=1}^{j} v\mu_k t_k < a\ , \quad j=1,2,\cdots,N. \tag{A.3}$$

These are written in the forms of the Fourier representation of the δ function and Dirichlet's discontinuity factor, respectively:

$$\frac{1}{2\pi}\int_{-\infty}^{\infty} d\rho \exp\left[i\rho\left(\sum_{j=1}^{N}\nu\mu_j t_j + \nu\mu\left(t-\sum_{j=1}^{N}t_j\right)-x\right)\right], \tag{A.4}$$

$$\frac{1}{\pi}\int_{-\infty}^{\infty} dx_j\, j_0(x_j)\exp\left[ix_j\left(\frac{2\nu}{a}\sum_{k=1}^{j}\mu_k t_k - 1\right)\right],\quad j=1,2,\cdots,N. \tag{A.5}$$

Then, introducing these conditions into Eq. (A.1), replacing x_j by $y_j=\frac{2}{\Sigma a}\sum_{k=j}^{N+1}x_k$ where x_{N+1} stands for $(a/2)\rho$, and integrating over μ_j $(j=2,3,\cdots,N)$ from -1 to 1 and over t_j $(j=1,2,\cdots,N)$ from 0 to $t-\sum_{k=1}^{j-1}t_k$, the number of neutrons with μ at x at time t as a result of the N-th collision, is obtained as follows:

$$n_N(x,\mu,t)=\left(\frac{\Sigma\nu}{2}\right)^N e^{-\Sigma\nu t}\frac{\Sigma}{2\pi}\int_{-\infty}^{\infty}dy_{N+1}\, e^{-i\Sigma(x-a/2)y_{N+1}}$$
$$\times\prod_{j=1}^{N}\left(\frac{c\Sigma a}{2\pi}\int_{-\infty}^{\infty}dy_j\, j_0\left[\frac{\Sigma a}{2}(y_j-y_{j+1})\right]\right)e^{-i\frac{\Sigma a}{2}y_1}H_N(t), \tag{A.6}$$

where $$H_N(t)=\int_0^t dt_1\, e^{i\Sigma\nu\mu_1 y_1 t_1}\prod_{j=2}^{N}\left(\int_0^{t-\sum_{k=1}^{j-1}t_k}dt_j\, 2j_0(\Sigma\nu y_j t_j)\right)e^{i\Sigma\nu\mu y_{N+1}\left(t-\sum_{j=1}^{N}t_j\right)}. \tag{A.7}$$

Now take the Laplace transform of $n_N(x,\mu,t)e^{\Sigma\nu t}$, then by applying the convolution theorem to $H_N(t)$ we have :

$$L_N(x,\mu,s)=\int_0^{\infty}dt\, e^{-st}n_N(x,\mu,t)e^{\Sigma\nu t}=\frac{\Sigma}{2\pi}\int_{-\infty}^{\infty}dy\,\frac{e^{-i\Sigma(x-a/2)y}}{s-i\Sigma\nu\mu y}F_N(y,s), \tag{A.8}$$

in which the independent variable y_{N+1} is replaced by y. The functions $F_j(y,s)$'s satisfy the following recurrence relation:

$$F_j(y,s)=\frac{c\Sigma a}{2\pi}\int_{-\infty}^{\infty}\frac{dz}{z}\tan^{-1}\left(\frac{\Sigma\nu z}{s}\right)j_0\left[\frac{\Sigma a}{2}(z-y)\right]F_{j-1}(z,s),$$
$$j=N,N-1,\cdots,2, \tag{A.9}$$

$$F_1(y,s)=\frac{c\Sigma a}{4\pi}\int_{-\infty}^{\infty}d\varrho\,\frac{e^{-i\frac{\Sigma a}{2}\varrho}}{s/(\Sigma v)-i\mu_1\varrho}\,j_0\left[\frac{\Sigma a}{2}(\varrho-y)\right].$$

For $N=0$, Eq. (A.8) is simplified to be

$$L_0(x,\mu,s)=\frac{1}{v\mu_1}\exp\left(-\frac{s}{v\mu_1}x\right)\delta(\mu-\mu_1). \qquad (A.10)$$

Let $L(x,\mu,s)$ be the Laplace transform of the number of neutrons with μ at x at time t coming from the ancestor neutron, multiplied by $e^{\Sigma vt}$, $n(x,\mu,t)e^{\Sigma vt}$, then according to Eq. (A.8)

$$\begin{aligned} L(x,\mu,s) &= \sum_{N=0}^{\infty} L_N(x,\mu,s) \\ &= L_0(x,\mu,s)+\frac{\Sigma}{2\pi}\int_{-\infty}^{\infty}dy\,\frac{e^{-i\Sigma(x-a/2)y}}{s-i\Sigma v\mu y}\,F(y,s), \end{aligned} \qquad (A.11)$$

where $F(y,s)=\sum_{N=1}^{\infty}F_N(y,s)$ obeys the following integral equation derived from Eq. (A.9):

$$F(y,s)=F_1(y,s)+\frac{c\Sigma a}{2\pi}\int_{-\infty}^{\infty}\frac{d\varrho}{\varrho}\tan^{-1}\left(\frac{\Sigma v\varrho}{s}\right)j_0\left[\frac{\Sigma a}{2}(\varrho-y)\right]F(\varrho,s). \qquad (A.12)$$

Upon integrating Eq. (A.11) with respect to μ, the Laplace transform of $n(x,t)e^{\Sigma vt}$, $L(x,s)$, is obtained in the form:

$$L(x,s)=\frac{1}{v\mu_1}\exp\left(-\frac{s}{v\mu_1}x\right)+\frac{1}{\pi v}\int_{-\infty}^{\infty}\frac{dy}{y}\exp\left[-i\Sigma(x-a/2)y\right]\tan^{-1}\left(\frac{\Sigma vy}{s}\right)F(y,s). \qquad (A.13)$$

And the Laplace transform of the total number of neutrons in the medium at time t multiplied by $e^{\Sigma vt}$, $n(t)e^{\Sigma vt}$, is derived by integrating Eq. (A.13) over x from 0 to a:

$$L(s)=\frac{1-e^{-as/(v\mu_1)}}{s}+\frac{a}{\pi v}\int_{-\infty}^{\infty}dy\,j_0\left(\frac{\Sigma a}{2}y\right)\frac{1}{y}\tan^{-1}\left(\frac{\Sigma vy}{s}\right)F(y,s). \qquad (A.14)$$

This equation together with Eq. (A.12) is nothing but that derived in the previous work (Asaoka, 1961).

Now $n(x,\mu,t)$ is reproduced by an inversion formula:

$$n(x,\mu,t)e^{\Sigma v t}=\frac{1}{2\pi i}\int_{\beta-i\infty}^{\beta+i\infty}ds\,e^{st}\,L(x,\mu,s)\,. \tag{A.15}$$

Let $\Sigma v s_1$ be the pole of $L(x,\mu,s)$, having the largest real part among those, and $R(x,\mu)$ the residue at $s=\Sigma v s_1$, then the asymptotic behaviour of $n(x,\mu,t)$ as $t\to\infty$ can be written as follows:

$$n(x,\mu,t)\sim R(x,\mu)\exp[(s_1-1)\Sigma v t]\,. \tag{A.16}$$

For the critical system, s_1 should be equal to unity and $vR(x,\mu)$ is no other than the vector flux.

Expanding $F(y,s)$ in the spherical Bessel functions:

$$F(y,s)=\sum_{n=0}^{\infty}b_n(s)j_n(\tfrac{\Sigma a}{2}y), \tag{A.17}$$

Eq. (A.15) is written in the following form according to Eq. (A.11):

$$n(x,\mu,t)e^{\Sigma v t}=\delta(x-v\mu_1 t)\delta(\mu-\mu_1)$$
$$+\sum_{n=0}^{\infty}\frac{\Sigma}{2\pi}\int_{-\infty}^{\infty}dy\exp[-i\Sigma(x-a/2)y]\,j_n(\tfrac{\Sigma a}{2}y)\frac{1}{2\pi i}\int_{\beta-i\infty}^{\beta+i\infty}ds\,\frac{b_n(s)}{s-i\Sigma v\mu y}e^{st}. \tag{A.18}$$

Consequently, it is seen that $s=\Sigma v s_1$ must be the pole of $b_m(s)$. Upon substituting Eq. (A.17) into Eq. (A.12), we arrive at an infinite set of linear equations obeyed by b_m, $b_m(s)$ with $s=\Sigma v s_1\,(s_1=1)$:

$$\frac{1}{c(2n+1)}b_n=\frac{\Sigma a}{2\mu_1}\exp(-\frac{\Sigma a}{2\mu_1})j_n(\frac{\Sigma a}{2i\mu_1})+\sum_{\substack{m=0\\ n+m=\text{even}}}^{\infty}b_m J(n,m), \tag{A.19}$$
$$n=0,1,2,\cdots.$$

Thus the condition that f_n should diverge beyond all bounds is that

$$\left|\frac{\delta_{nm}}{(2n+1)C}-J(nm)\right|=0, \qquad n,m = 0,2,4,\cdots \quad \text{or} \quad 1,3,5,\cdots\ . \tag{A.20}$$

This coincides with Eq. (10) in the text, and hence following the same consideration as in the text it is concluded that only the determinant with even values for both n and m shall vanish and this gives the critical condition.

From Eq. (A.18), the residue at $s=\Sigma v$, $R(x,\mu)$, is thus given by

$$R(x,\mu)=\frac{1}{2\pi v}\sum_{m=0}^{\infty} f_{2m}\int_{-\infty}^{\infty}dy\,\frac{\exp[-i\Sigma(x-a/2)y]}{1-i\mu y}\,j_{2m}\left(\frac{\Sigma a}{2}y\right), \tag{A.21}$$

of which the coefficients f_{2m}'s are to be determined by Eq. (11) in the text, as easily seen from Eq. (A.19) together with Eq. (A.20) with even values for both n and m. This is nothing but Eq. (12).

Appendix 2. Formulation Based on the Neutron-Balance Viewpoint

Here we shall consider the correspondence between our formulation based on the life-cycle viewpoint and the transport equation governing the balance of neutrons.

In order to derive the transport equation from the conservation of neutrons, consideration will be given to $n(x,\mu,t)\,dx\,d\mu$, the number of neutrons in dx at x, with directional cosines between μ and $\mu+d\mu$ at time t, within a critical slab into the surface of which, $x=0$, one neutron with μ_1 has been shot at time $t=0$.

The number of neutrons in $d\mu$ at μ produced as a result of collisions in $d\chi'$ at χ', in dt' at time $t-t'$, is given by

$$\frac{c\Sigma v}{2}\left(\int_{-1}^{1} d\mu' n(\chi', \mu', t-t')\right) d\chi' dt' d\mu .$$

The probability that the neutrons travel for a time t' without further collision is $e^{-\Sigma v t'}$ and the space coordinate after the travel is $\chi' + v\mu t'$. Since we are interested in $n(\chi, \mu, t) d\chi d\mu$, the following condition must be taken into account in order to fix the observing point in $d\chi$ at χ :

$$\chi - \tfrac{1}{2}d\chi < \chi' + v\mu t' < \chi + \tfrac{1}{2}d\chi .$$

This condition is rewritten in the form:

$$\begin{aligned}\frac{1}{\pi}\int_{-\infty}^{\infty} d\rho \frac{\sin \frac{1}{2}d\chi\rho}{\rho} \exp[i\rho(\chi' + v\mu t' - \chi)] \\ = d\chi \frac{\Sigma}{2\pi}\int_{-\infty}^{\infty} d\varrho \exp[i\Sigma\varrho(\chi' + v\mu t' - \chi)] ,\end{aligned} \tag{A.22}$$

and hence $n(\chi, \mu, t)$ is given as follows:

$$\begin{aligned} n(\chi, \mu, t) &= \delta(\chi - v\mu_1 t)\delta(\mu - \mu_1) e^{-\Sigma v t} \\ &+ \frac{c\Sigma v}{2}\int_0^a d\chi' \int_0^t dt' \frac{\Sigma}{2\pi}\int_{-\infty}^{\infty} d\varrho \exp[i\Sigma\varrho(\chi' + v\mu t' - \chi)] e^{-\Sigma v t'} \int_{-1}^{1} d\mu' n(\chi', \mu', t-t') .\end{aligned} \tag{A.23}$$

Now we shall derive Eq. (A.11) from this transport equation. First of all, take the Laplace transform of both the sides of Eq. (A.23) multiplied by $e^{\Sigma v t}$, then we have

$$\begin{aligned} L(\chi, \mu, s) &= \frac{1}{v\mu_1} \exp\left(-\frac{s}{v\mu_1}\chi\right)\delta(\mu - \mu_1) \\ &+ \frac{\Sigma}{2\pi}\int_{-\infty}^{\infty} d\varrho \frac{e^{-i\Sigma\chi\varrho}}{s - i\Sigma v\mu\varrho} \frac{c\Sigma v}{2}\int_0^a d\chi' e^{i\Sigma\varrho\chi'} \int_{-1}^{1} d\mu' L(\chi', \mu', s) .\end{aligned} \tag{A.24}$$

Further, upon integrating Eq. (A.24) over μ, we get

$$L(\chi, s) = \frac{1}{v\mu_1} \exp\left(-\frac{s}{v\mu_1}\chi\right) + \frac{c\Sigma}{2\pi}\int_{-\infty}^{\infty} \frac{d\varrho}{\varrho} \tan^{-1}\left(\frac{\Sigma v \varrho}{s}\right) e^{-i\Sigma\chi\varrho} \int_0^a d\chi' e^{i\Sigma\varrho\chi'} L(\chi', s). \tag{A.25}$$

This leads to

$$\int_0^a dx\, e^{i\Sigma y x} L(x,s) = \frac{1-\exp\left(-\frac{sa}{v\mu_1}\right) e^{i\Sigma a y}}{s - i\Sigma v \mu_1 y}$$

$$+ \frac{c\Sigma a}{2\pi} \int_{-\infty}^{\infty} \frac{dz}{z} \tan^{-1}\left(\frac{\Sigma v z}{s}\right) j_0\left[\frac{\Sigma a}{2}(y-z)\right] \exp\left[i\frac{\Sigma a}{2}(y-z)\right] \int_0^a dx' e^{i\Sigma z x'} L(x',s). \quad \text{(A.26)}$$

This equation is nothing but Eq. (A.12) as immediatly seen if we introduce the following representation:

$$F(y,s) = \frac{c\Sigma v}{2} e^{-i\frac{\Sigma a}{2}y} \int_0^a dx\, e^{i\Sigma y x} L(x,s), \quad \text{(A.27)}$$

and then further Eq. (A.24) is reduced to Eq. (A.11). Equation (A.27) tells us also that

$$F(0,s) = \frac{c\Sigma v}{2} L(s), \quad \text{(A.28)}$$

which has been already shown in the previous work (Asaoka, 1961).

As seen from the above-mentioned formulation, the essential point of our technique is not only the adoption of a viewpoint different from the usual one but also the introduction of the discontinuity factors such as Eq. (A.22). As a result of this, the neutron transport problems for a finite system can be dealt with in a similar way as those for an infinite system.

Appendix 3. Critical Condition and Flux Distribution for Bare Spheres

The determination of the flux distribution in spherically symmetric systems, as well known, can be reduced to its determination in a certain system with plane symmetry. Actmally, this is shown easily by following a similar procedure as in Appendix 2.

Let r be the radial coordinate and μ the cosine of the angle between the neutron velocity and the direction of r. The number of neutrons in $d\mu_0$ at μ_0 produced as a result of collisions in $4\pi r'^2 dr'$ at r', in dt' at time $t-t'$, is given by

$$\frac{c\Sigma v}{2} n(r', t-t') 4\pi r'^2 dr' dt' d\mu_0 .$$

Taking account of the condition,

$$r^2 = r'^2 + (vt')^2 + 2r' v\mu_0 t',$$

the number of neutrons in $4\pi r^2 dr$ at r at time t is written as follows:

$$n(r,t) 4\pi r^2 dr = \frac{c\Sigma v}{2}\int_0^R dr' 4\pi r'^2 \int_0^t dt' \int_{-1}^{1} d\mu_0 n(r', t-t') e^{-\Sigma v t'}$$

$$\times\left[\delta\left(\sqrt{r'^2+(vt')^2+2r'v\mu_0 t'}-r\right)+\delta\left(\sqrt{r'^2+(vt')^2+2r'v\mu_0 t'}+r\right)\right]dr, \qquad (A.29)$$

where R is the radius of the sphere and the source neutron at time $t=0$ is omitted because our interest lies in the asymptotic behaviour of $n(r,t)$ as $t\to\infty$.

Now replacing μ_0 by $\zeta=\sqrt{r'^2+(vt')^2+2r'v\mu_0 t'}$, rewritting $\delta(\zeta-r)$ in the form of $\frac{1}{2\pi}\int_{-\infty}^{\infty} d\rho \exp[i\rho(\zeta-r)]$, integrating over ζ from $|r'-vt'|$ to $r'+vt'$ and taking the Laplace transform, then we have :

$$r^2 L(r,s) = r^2\int_0^\infty dt\, e^{-st} n(r,t) e^{\Sigma v t}$$

$$= -i\frac{c\Sigma}{2\pi}\int_{-\infty}^{\infty} d\rho\, e^{-i\rho r}\frac{d}{d\rho}\left[\frac{1}{\rho}\tan^{-1}\frac{\rho v}{s}\int_0^R dr' r'(e^{i\rho r'}-e^{-i\rho r'})L(r',s)\right]. \qquad (A.30)$$

This leads to

$$\gamma L(\gamma,s)=\frac{c\Sigma}{2\pi}\int_{-\infty}^{\infty}d\rho\, e^{-i\rho\gamma}\frac{1}{\rho}\tan^{-1}\frac{\rho v}{s}\int_{0}^{R}d\gamma'\gamma'(e^{i\rho\gamma'}-e^{-i\rho\gamma'})L(\gamma',s),$$

or extending the definition of $L(\gamma,s)$ to $\gamma<0$ by putting $L(-\gamma,s)=L(\gamma,s)$,

$$\gamma L(\gamma,s)=\frac{c\Sigma}{2\pi}\int_{-\infty}^{\infty}\frac{d\vartheta}{\vartheta}\tan^{-1}\left(\frac{\Sigma v\vartheta}{s}\right)e^{-i\Sigma\vartheta\gamma}\int_{-R}^{R}d\gamma' e^{i\Sigma\vartheta\gamma'}\gamma' L(\gamma',s), \tag{A.31}$$

in which ρ is replaced by $\vartheta=\rho/\Sigma$.

From this equation, we get :

$$F(y,s)=\frac{c\Sigma R}{\pi}\int_{-\infty}^{\infty}\frac{d\vartheta}{\vartheta}\tan^{-1}\left(\frac{\Sigma v\vartheta}{s}\right)j_0[\Sigma R(y-\vartheta)]\,F(\vartheta,s), \tag{A.32}$$

where

$$F(y,s)=\frac{c\Sigma v}{2}\int_{-R}^{R}d\gamma\, e^{i\Sigma y\gamma}\gamma L(\gamma,s). \tag{A.33}$$

And by combining Eqs. (A.31) and (A.33), we have :

$$\gamma L(\gamma,s)=\frac{1}{\pi v}\int_{-\infty}^{\infty}\frac{d\vartheta}{\vartheta}\tan^{-1}\left(\frac{\Sigma v\vartheta}{s}\right)e^{-i\Sigma\gamma\vartheta}F(\vartheta,s). \tag{A.34}$$

This can be identified with Eq. (A.13) omitted the source term, because Eq. (A.13) is rewritten in the following form when the origin of the space coordinate is displaced to the center of the slab:

$$L(x,s)=\frac{1}{\pi v}\int_{-\infty}^{\infty}\frac{dy}{y}\tan^{-1}\left(\frac{\Sigma v y}{s}\right)e^{-i\Sigma x y}F(y,s), \tag{A.13'}$$

and besides Eq. (A.32) is identified at once with Eq. (A.12), upon omitting the source term which comes from the neutrons undergoing the first collision. That is, Eq. (A.34) together with Eq. (A.32) is nothing but the equation governing the neutron distribution in a slab of thickness $2R$,where $rn(r,t)$ is the neutron flux.

Now expanding $F(y,s)$ in the spherical Bessel functions:

$$F(y,s)=\sum_{m=0}^{\infty} f_m(s) j_m(\Sigma R y), \qquad (A.35)$$

it is immediately seen that only the terms with odd values of m in this infinite series remain on the right side of Eq. (A.34), contrary to the case of Eq. (A.13'), because $rL(r,s)$ should be an odd function about r and hence the coefficient of $F(z,s)$ in the integrand of Eq. (A.34) should be an odd function about z .

Thus, $n(r,t)$ is written in the form according to Eqs. (A.34) and (A.35):

$$rn(r,t)e^{\Sigma vt}=\frac{1}{\pi v}\sum_{m=0}^{\infty}\int_{-\infty}^{\infty}\frac{dz}{z}e^{-i\Sigma rz} j_{2m+1}(\Sigma Rz)\frac{1}{2\pi i}\int_{\beta-i\infty}^{\beta+i\infty} ds\, e^{st}\tan^{-1}\left(\frac{\Sigma vz}{s}\right) f_{2m+1}(s). \qquad (A.36)$$

Since $s=\Sigma v$ must be the pole of $f_{2m+1}(s)$ for the critical system, the neutron distribution in the critical shere is given by

$$rn(r)=\frac{1}{\pi v}\sum_{m=0}^{\infty} f_{2m+1}\int_{-\infty}^{\infty} dz\, e^{-i\Sigma rz}\,\frac{\tan^{-1}z}{z}\, j_{2m+1}(\Sigma Rz), \qquad (A.37)$$

where f_{2m+1} is the residue of $f_{2m+1}(s)$ at $s=\Sigma v$. Performing the integration, this becomes :

$$\begin{aligned} rvn(r)=\sum_{m=0}^{\infty} f_{2m+1}\Big\{ & iR\left[\frac{\tan^{-1}z}{z} j^{1}_{2m+1}(\Sigma Rz)\left(e^{i\Sigma(R-r)z}-e^{i\Sigma(R+r)z}\right)\right]_{z=0} \\ & +\int_{1}^{\infty}\frac{dt}{t} j^{1}_{2m+1}(i\Sigma Rt)\left(e^{-\Sigma(R-r)t}-e^{-\Sigma(R+r)t}\right)\Big\}, \end{aligned} \qquad (A.38)$$

where $j_{2m+1}(z)=j^{1}_{2m+1}(z)e^{iz}+j^{2}_{2m+1}(z)e^{-iz} \quad \left(j^{2}_{2m+1}(z)=-j^{1}_{2m+1}(-z)\right)$.

The concrete expression up to in the j_3-approximation is :

$$\frac{i\alpha R}{f_1} v n(\xi) = 1 - \frac{\alpha}{2\xi} E_2'' - \frac{1}{2\xi} E_3'' \\ - \left(-\frac{3}{2} + \frac{5}{2}\frac{\xi^2}{\alpha^2} + \frac{5}{\alpha^2} - \frac{\alpha}{2\xi} E_2'' - \frac{3}{\xi} E_3'' - \frac{15}{2\alpha\xi} E_4'' - \frac{15}{2\alpha^2\xi} E_5'' \right) \frac{f_3}{f_1} , \tag{A.39}$$

where $\alpha = \Sigma R$, $\xi = \Sigma r$ and $E_n'' = E_n(\alpha-\xi) - E_n(\alpha+\xi)$.

On the other hand, $f_{2n+1}(s)$'s with $s = \Sigma v$ obey the following infinite set of linear equations which are derived by substituting Eq. (A.35) into Eq. (A.32):

$$\frac{1}{(4m+3)c} f_{2m+1}(\Sigma v) = \sum_{n=0}^{\infty} f_{2n+1}(\Sigma v) J(2m+1, 2n+1), \qquad m = 0, 1, 2, \cdots , \tag{A.40}$$

and hence the critical condition is given by

$$\left| \frac{\delta_{nm}}{c(4m+3)} - J(2m+1, 2n+1) \right| = 0, \quad n, m = 0, 1, 2, \cdots , \tag{A.41}$$

where

$$J(2m+1, 2n+1) = \frac{2\alpha}{\pi} \int_0^{\infty} dy\, j_{2m+1}(\alpha y) j_{2n+1}(\alpha y) \frac{\tan^{-1} y}{y} .$$

The ratios among the values of f_{2m+1}'s are determined as follows:

$$f_1 : f_3 : f_5 : \cdots$$

$$= \begin{vmatrix} -J(1,3) & -J(1,5) & -J(1,7)\cdots \\ \frac{1}{7c} - J(3,3) & -J(3,5) & \\ -J(5,3) & \frac{1}{11c} - J(5,5) & \\ \vdots & & \end{vmatrix} : \begin{vmatrix} -\frac{1}{3c} + J(1,1) & -J(1,5) & -J(1,7)\cdots \\ J(3,1) & -J(3,5) & \\ J(5,1) & \frac{1}{11c} - J(5,5) & \\ \vdots & & \end{vmatrix} : \begin{vmatrix} -J(1,3) & -\frac{1}{3c} + J(1,1) & -J(1,7)\cdots \\ \frac{1}{7c} - J(3,3) & J(3,1) & \\ -J(5,3) & J(5,1) & \\ \vdots & & \end{vmatrix} : \cdots . \tag{A.42}$$

In accordance with Eq. (A.41), the critical conditions in the j_1- and the j_3-approximation are written in the following forms, respectively:

(a) The j_1-approximation;

$$\frac{1}{C}=3J(1,1)\sim\begin{cases}\frac{3}{4}\alpha\left(1-\frac{8}{15}\alpha\right), & \alpha\ll 1,\\ 1-\frac{3}{4\alpha}+\frac{3}{8\alpha^3}, & \alpha\gg 1,\end{cases} \tag{A.43}$$

(b) The j_3-approximation;

$$\frac{1}{C}=\frac{3}{2}J(1,1)+\frac{7}{2}J(3,3)+\sqrt{\left(\frac{3}{2}J(1,1)-\frac{7}{2}J(3,3)\right)^2+21\left(J(1,3)\right)^2}$$

$$\sim\begin{cases}\frac{5}{144}(15+\sqrt{57})\alpha\left(1-\frac{432972+26060\sqrt{57}}{1246875}\alpha\right) \\ \qquad =0.78298\alpha(1-0.50504\alpha), \quad \alpha\ll 1,\\ 1-\frac{7}{2\alpha^2}+\frac{1799}{240\alpha^3}, \quad \alpha\gg 1.\end{cases} \tag{A.44}$$

The expression of $3J(1,1)$ is the same as that of the collision probability on first flight under the assumption of the uniform neutron distribution within the sphere (Case et al., 1953), like the expression of $1/C$ in the j_0-approximation for the critical slab is the same as that of the collision probability for the uniform distribution within the slab (Asaoka, 1961).

The values of C for various values of $\Sigma R=\alpha$ between 0.005 and 50 are shown in Table A.1. Our results are compared with Carlson's work, in which he obtained the critical radius for various values of C by using a quadratic trial function in the single-iteration moments method (Carlson, 1949). As seen from Fig. A.2, our results in the j_3-approximation are on the curve showing his results.

Case K.M., Hoffmann F. and Placzek G. (1953) - Introduction to the Theory of Neutron Diffusion, Vol.1, Sec. 10.2.

Carlson B. (1949) - Neutron Diffusion Theory; Integral Theory Methods and Formulae, AECD-2835 (LA-990), or see Reactor Handbook, Vol.III, Part A, Chap.4, 154 (1962).

And further, the so-called extrapolation distance d has been calculated according to the following form:

$$\Sigma d = \frac{\pi}{\sqrt{3(1-V_c)}} - \Sigma R, \tag{A.45}$$

which, upon substituting Eq. (A.43) or (A.44), gives:

(a) The j_1-approximation;

$$\Sigma d \sim \begin{cases} \pi/\sqrt{3} - (1 - \pi\sqrt{3}/8)\alpha, & \alpha \ll 1, \\ (2\pi/3)\sqrt{\alpha} - \alpha, & \alpha \gg 1, \end{cases} \tag{A.46}$$

(b) The j_3-approximation;

$$\Sigma d \sim \begin{cases} \frac{\pi}{\sqrt{3}} - \left(1 - 5\pi\frac{5\sqrt{3}+\sqrt{19}}{288}\right)\alpha, & \alpha \ll 1, \\ -\left(1 - \frac{2}{\sqrt{42}}\pi\right)\alpha + \frac{257}{120}\frac{\pi}{\sqrt{42}} = -0.030483\alpha + 1.03819, & \alpha \gg 1. \end{cases} \tag{A.47}$$

The values of Σd corresponding to each value of the critical radius R are shown in Table A.1.

Also from this Table, it is seen that the accuracy of the results in the j_1- and the j_3-approximation may be in the same extent as that of the results in the j_0- and the j_2-approximation, respectively, for the case of the slab (Asaoka, 1961). And hence it may be believed that our results in the j_3-approximation are accurate, except the extrapolation distance for the spheres with very large radius, of which even the error around 0.001% for c might give an influence on the first figure of the value of Σd .

In the j_3-approximation, the ratio of b_3 to b_1 is given in the following form according to Eq. (A.42), together with Eq. (A.44):

$$\frac{b_3}{b_1} = \frac{1/(3c) - J(1,1)}{J(1,3)} = \frac{J(1,3)}{1/(7c) - J(3,3)}$$

$$\sim \begin{cases} \frac{5\sqrt{57}-33}{12}\left(1 + \frac{2012\sqrt{57}}{35625}\alpha\right) = 0.39576\,(1 + 0.4264\alpha), & \alpha \ll 1, \\ 1 - 4/(3\alpha), & \alpha \gg 1. \end{cases} \tag{A.48}$$

Then for small α, the leading term of the right side of Eq. (A.39) is given as follows:

(a) The j_1-approximation;

$$\frac{i\alpha R}{k_1} vn(\xi) \sim \begin{cases} \alpha\left(1-\frac{1}{3}\frac{\xi^2}{\alpha^2}\right), & \xi \ll 1, \\ \frac{\alpha}{2}+\frac{1}{2}\ln\left(\frac{2\alpha}{\xi_0}\right)\xi_0, & \xi_0=\alpha-\xi \ll 1, \end{cases} \tag{A.49}$$

(b) The j_3-approximation;

$$\frac{i\alpha R}{k_1} vn(\xi) \sim \begin{cases} \frac{5}{18}(\sqrt{57}-3)\alpha\left(1-\frac{25+3\sqrt{57}}{8}\frac{\xi^2}{\alpha^2}\right) \\ \qquad = 1.263840\alpha\left(1-5.9562\frac{\xi^2}{\alpha^2}\right), & \xi \ll 1, \\ \frac{5}{144}(21-\sqrt{57})\alpha+\frac{5}{24}(9-\sqrt{57})\left(\ln\frac{2\alpha}{\xi_0}+\frac{\sqrt{57}-1}{4}\right)\xi_0 \\ \qquad = 0.467020\alpha+0.30212\left(\ln\frac{2\alpha}{\xi_0}+1.6375\right), & \xi_0=\alpha-\xi \ll 1. \end{cases}$$

(A.50)

And for large α,

(a) The j_1-approximation;

$$\frac{i\alpha R}{k_1} vn(\xi) \sim \begin{cases} 1, & \xi \ll 1, \\ \frac{1}{2}-\frac{1}{4\alpha}+\frac{1}{2}\left(\ln\frac{1}{\xi_0}-\gamma+1\right)\xi_0, & \xi_0=\alpha-\xi \ll 1, \end{cases} \tag{A.51}$$

(b) The j_3-approximation;

$$\frac{i\alpha R}{k_1} vn(\xi) \sim \begin{cases} \frac{5}{2}-\frac{2}{\alpha}-\frac{5}{\alpha^2}-\frac{5}{2}\left(\frac{\xi}{\alpha}\right)^2, & \xi \ll 1, \\ \frac{23}{12\alpha}+\frac{2}{3\alpha}\left(\ln\frac{1}{\xi_0}-\gamma+\frac{17}{2}\right)\xi_0, & \xi_0=\alpha-\xi \ll 1. \end{cases} \tag{A.52}$$

Similarly to the case of the slab shown in the text, the results converge fast for the smaller values of α as going to the higher order approximation, but not so faster for larger α.

The extrapolated end-point $-\xi_0$ is obtained from the following equation according to Eqs. (A.38) and (A.39):

$$1-\left[-\frac{3}{2}+\frac{5}{2}\left(1-\frac{\xi_0}{\alpha}\right)^2+\frac{5}{\alpha^2}\right]\frac{k_3}{k_1}=0. \tag{A.53}$$

For large α , this gives in the j_3-approximation that

$$-\xi_0 = 4/15. \tag{A.54}$$

From the results shown so far, together with those in the j_2-approximation in Fig. 5, we are convinced that our results of the flux distribution in the j_3-approximation are practically regarded as the accurate ones, whether the radius of the sphere is large or small. In Fig. A.3 are shown the results for the spheres with α=0.005,0.5 and 10.

In this Appendix, thus, we have got the values of C required to keep the bare sphere to be critical, within an error less than 0.01%. And the values of the extrapolation distance, which are indispensable to evaluate the critical condition by means of the elementary diffusion theory, have been obtained accurately for the system with radius less than several times of the neutron mean free path. Besides these, the flux distribution within the critical sphere has been derived also in a concise form to be calculated easily.

Table A.1 —— The Mean Number of Secondaries per Collision and the Extrapolation Distance for the Critical Sphere of Radius R

Radius ΣR	Mean number of secondaries C		Extrapolation distance Σd	
	j_1-approximation	j_3-approximation	j_1-approximation	j_3-approximation
0.005	267.378	256.080	1.8122	1.8124
0.05	27.3819	26.1915	1.7979	1.7995
0.25	6.06442	5.77785	1.7348	1.7446
0.5	3.41620	3.23743	1.6567	1.6818
1	2.11529	1.98870	1.4979	1.5724
2	1.49794	1.39634	1.1459	1.4045
5	1.172335	1.096470	-0.2693	1.1149
10	1.080643	1.028710	-4.3603	0.8572
50	1.015225	1.001342	-36.1889	-0.4602

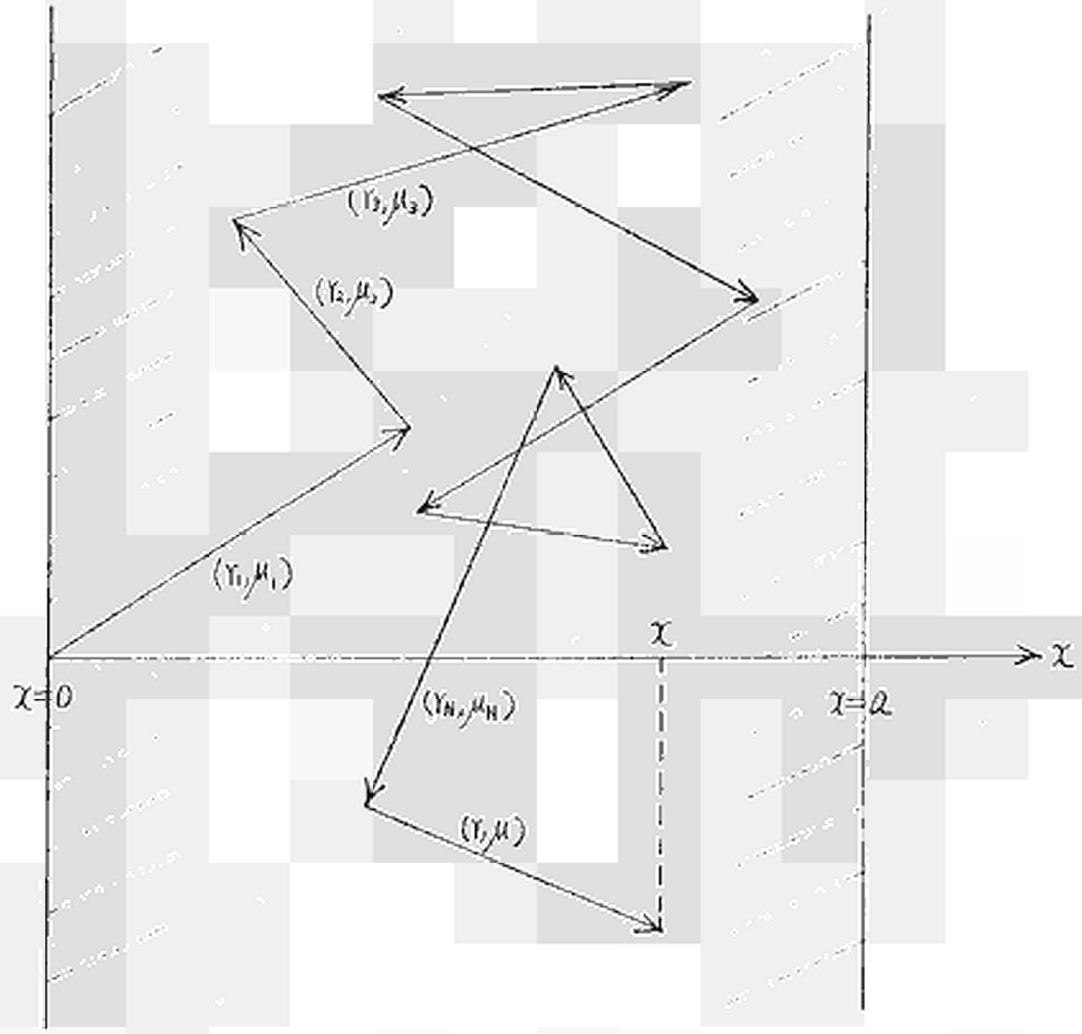

Fig. 1 —— A typical path of the neutron in the slab of thickness a

Fig. 2 — The vector flux at $\Sigma x=0$ and 0.005 in the slab with $\Sigma a=0.01$

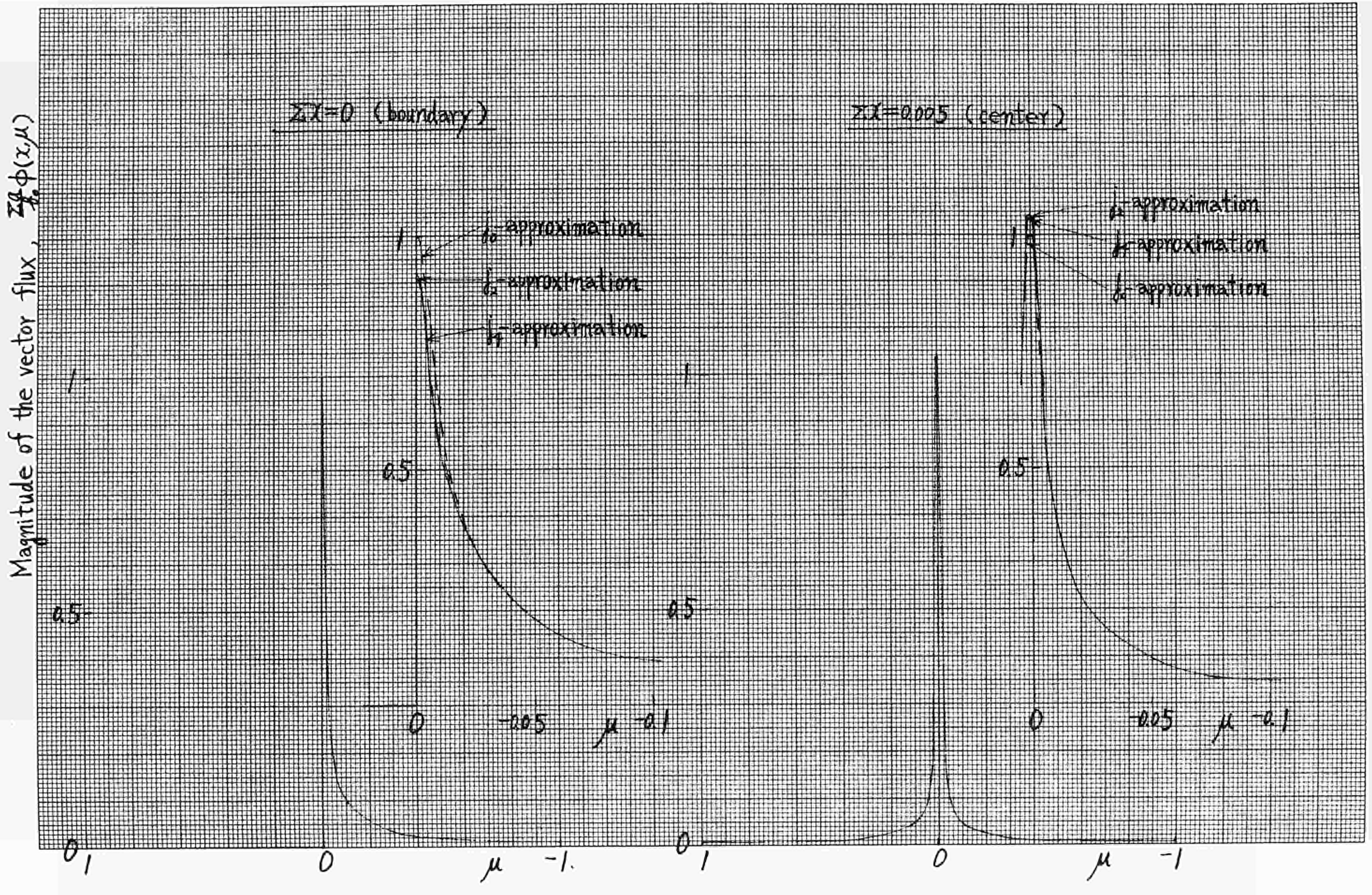

Fig. 4 — The vector flux at $\Sigma x=0, 1, 4$ and 10 in the slab with $\Sigma a=20$

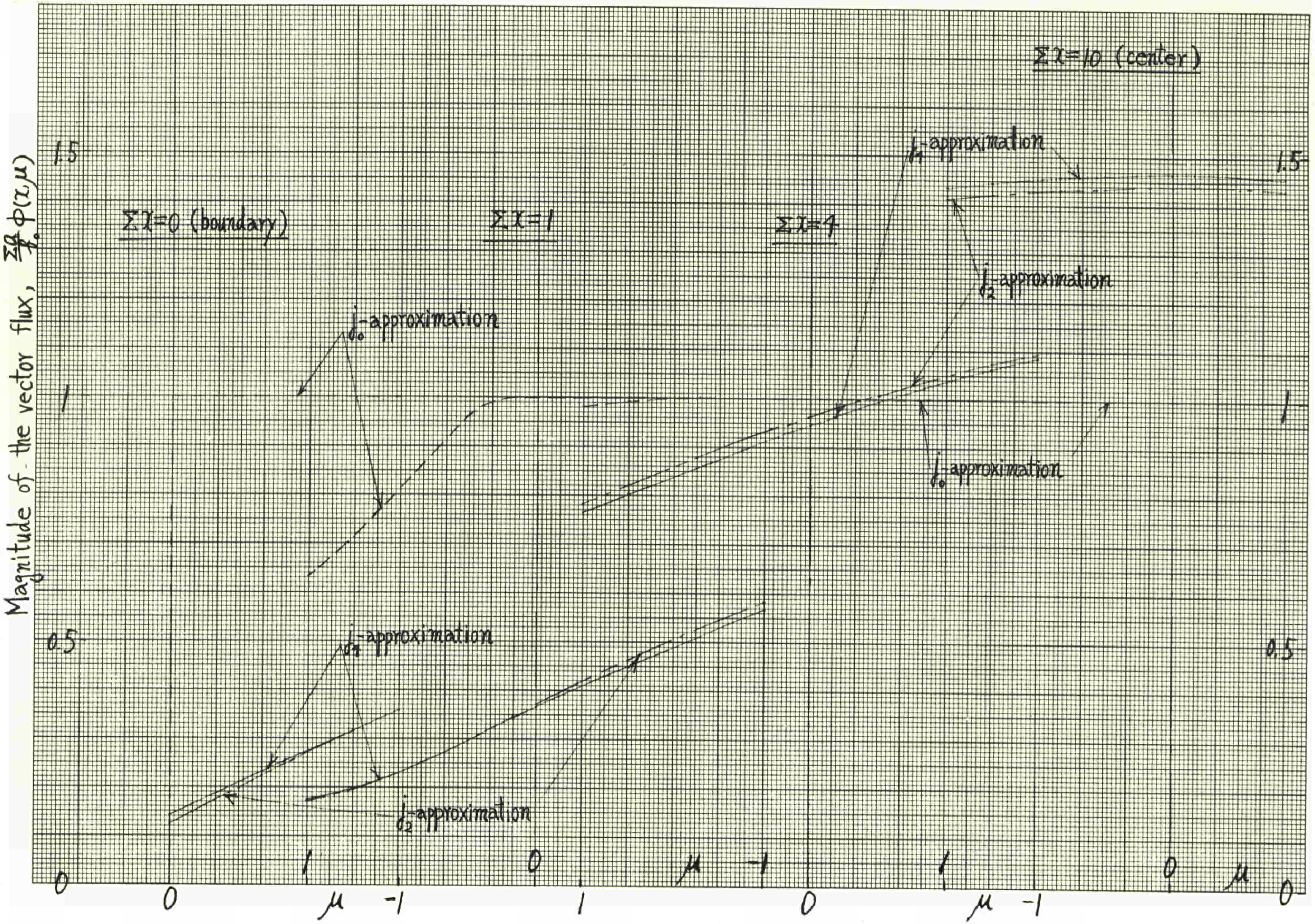

Fig. 4 — The vector flux at $\Sigma x=0, 1, 4$ and 10 in the slab with $\Sigma a=20$

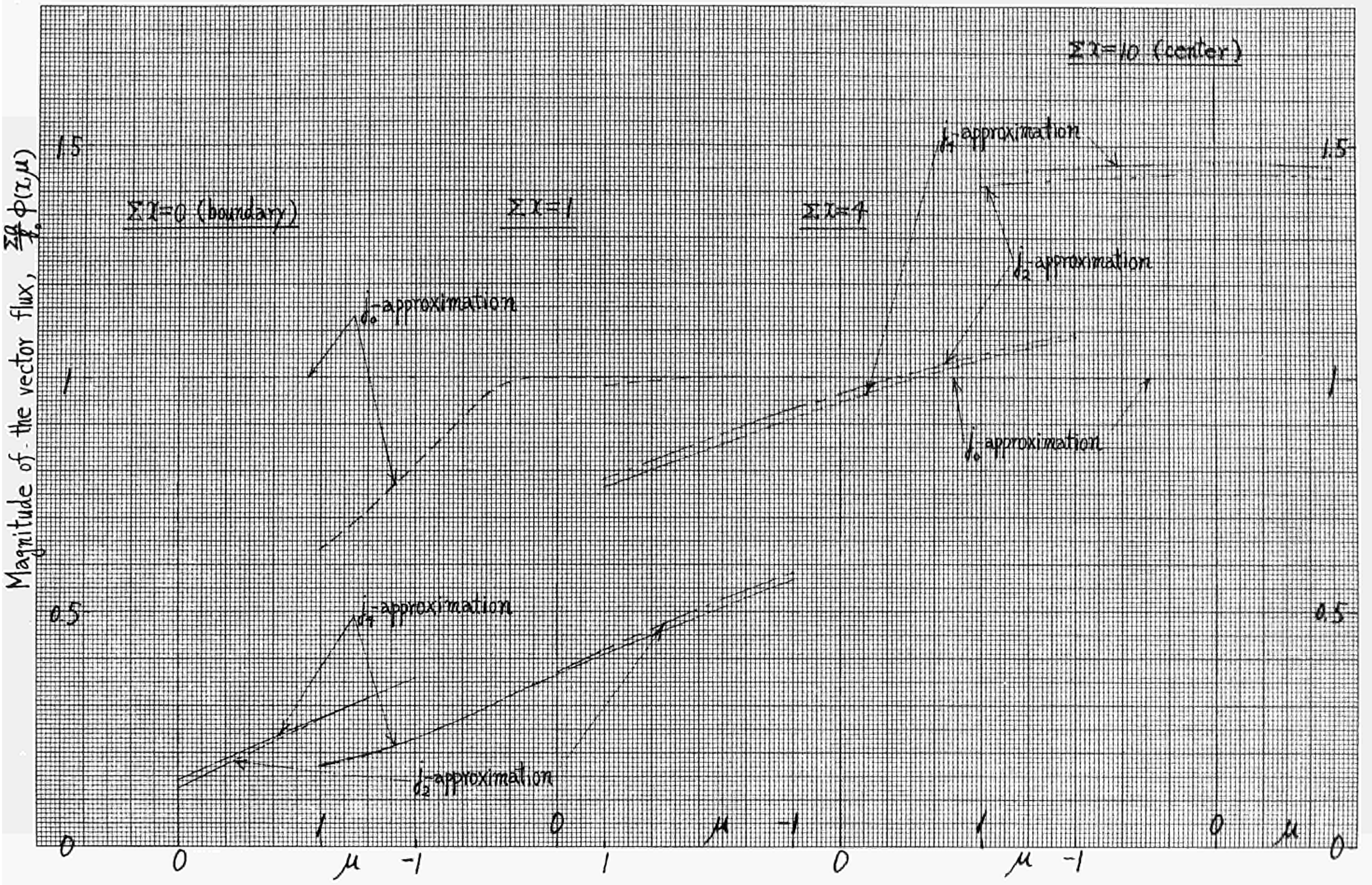

Fig. 5 — The scalar flux within the slab of thickness $\Sigma a = 0.01$, 1 and 20

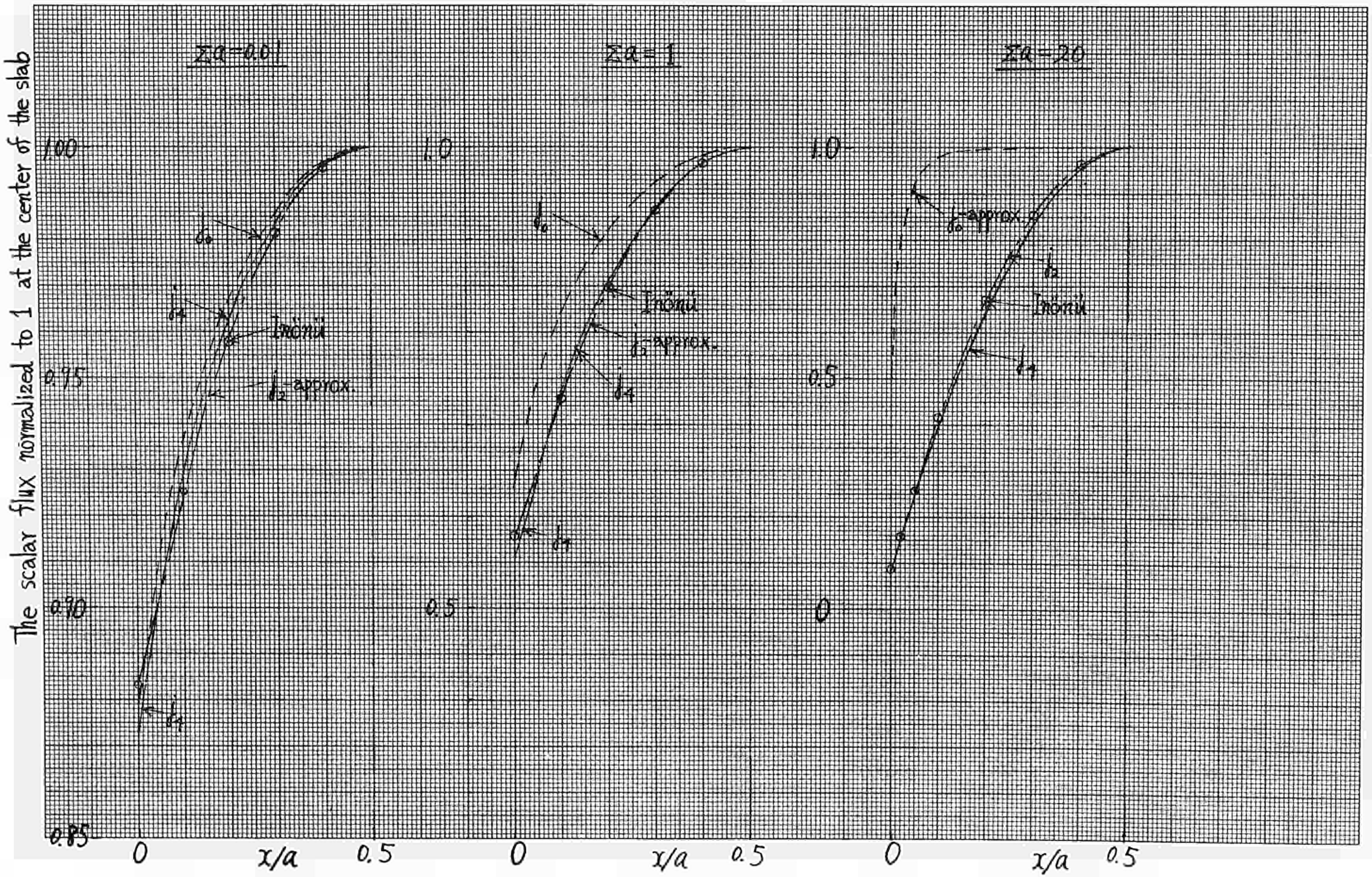

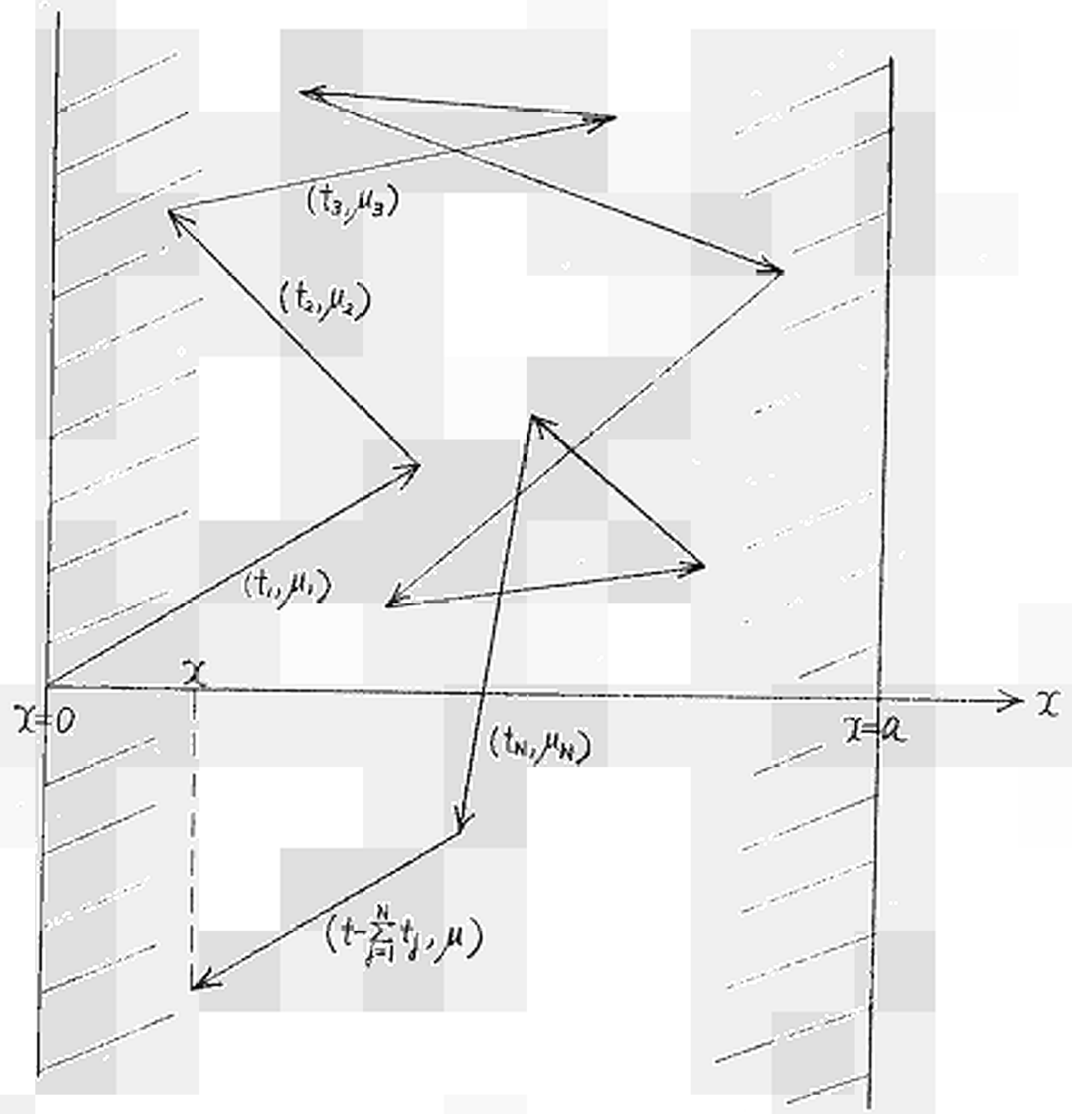

Fig. A.1 —— A typical path of the neutron in the slab of thickness a

Fig. A·2 — Comparison of our results for the mean number of secondaries per collision for the critical sphere of radius R, with Carlson's

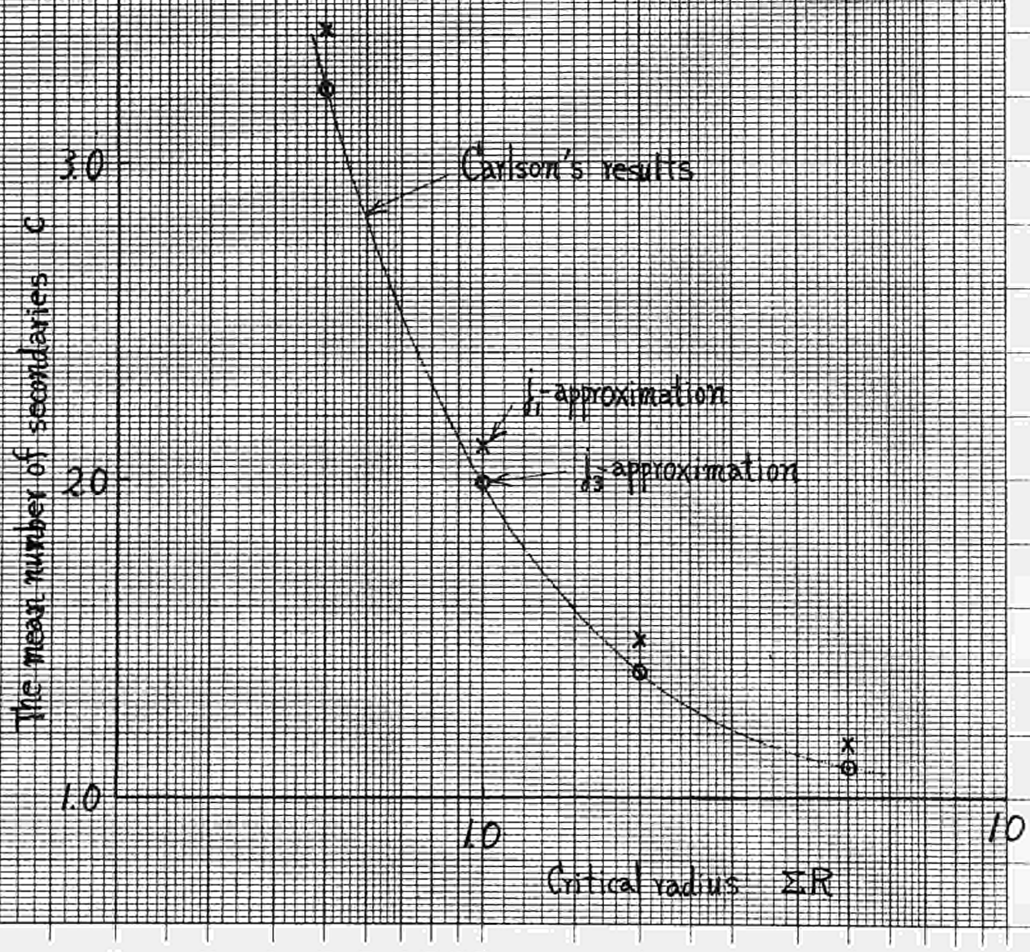

Logar. Teilung / Division } 1-100, Einheit / Unité } 83,33 mm
Ed. Aerni-Leuch, Bern Nr. 527

Fig. A·3 — The flux distribution within the critical sphere with radius $\Sigma R = 0.005$, 0.5 and 10

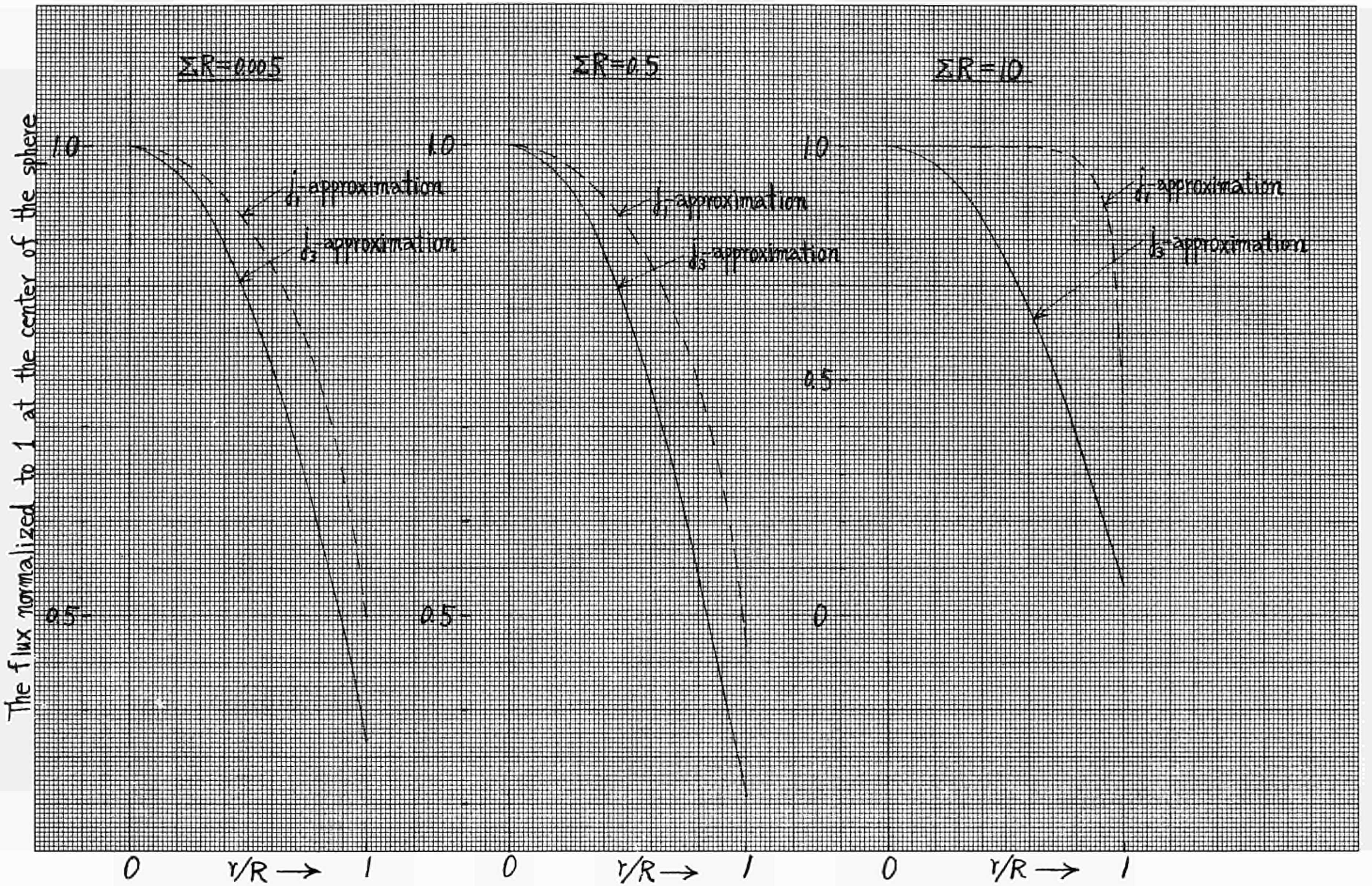

CDNA00479ENC